JCI insight

Preclinical assessment of oral TLR7 agonist SA-5 in a non-human primate model

Shokichi Takahama, Takahiro Tomiyama, Sachiyo Yoshio, Yuta Nagatsuka, Hirotomo Murakami, Takuto Nogimori, Mami Kochi, Shoko Ochiai, Hidenori Kimura, Akihisa Fukushima, Tatsuya Kanto, Takuya Yamamoto

JCI Insight. 2025. https://doi.org/10.1172/jci.insight.196809.

Research In-Press Preview **Hepatology** **Immunology** **Infectious disease**

Toll-like receptor 7 (TLR7) agonists are promising immunostimulatory agents for the treatment of chronic infections and cancer. However, their systemic toxicity remains a challenge. In this study, SA-5, a novel liver-targeted, orally available TLR7 agonist, was evaluated for pharmacokinetics, safety, and efficacy in young and aged macaques across 1–10 mg/kg repeated doses. Safety was evaluated through hematologic, biochemical, and flow cytometric profiling, while efficacy was assessed via IFN-α production, gene expression of interferon-stimulated genes, and plasmacytoid dendritic cell activation. A principal component analysis (PCA)-based composite scoring system was used to integrate multimodal parameters. SA-5 induced dose-dependent type I IFN with limited systemic inflammation, with 3 mg/kg showing optimal balance. SA-5 had comparable immunostimulatory activity to GS-9620 but with reduced adverse biomarker shifts. In aged macaques, efficacy was maintained with modestly increased safety responses. These findings support SA-5 as a safer next-generation TLR7 agonist effective across age groups, highlighting integrated biomarker profiling in preclinical immunomodulatory drug development.

Preclinical assessment of oral TLR7 agonist SA-5 in a non-human primate model

Shokichi Takahama[1#], Takahiro Tomiyama[1#], Sachiyo Yoshio[2], Yuta Nagatsuka[1], Hirotomo Murakami[1], Takuto Nogimori[1], Mami Kochi[3], Shoko Ochiai[3], Hidenori Kimura[3], Akihisa Fukushima[3], Tatsuya Kanto[4] and Takuya Yamamoto[1, 5, 6, 7*]

[1]Laboratory of Precision Immunology, Center for Intractable Diseases and ImmunoGenomics, National Institutes of Biomedical Innovation, Health and Nutrition, Osaka 567-0085, Japan.

[2]Department of Human Immunology and Translational Research, National Institute of Global Health and Medicine, Japan Institute for Health Security, Tokyo 162-8655, Japan.

[3]Research and Development (Division), Sumitomo Pharma. Co., Ltd., Osaka, 554-0022, Japan.

[4]Department of Liver Diseases, The Research Center for Hepatitis and Immunology, National Institute of Global Health and Medicine, Japan Institute for Health Security, Chiba 272-8516, Japan.

[5]Laboratory of Aging and Immune Regulation, Graduate School of Pharmaceutical Sciences, The University of Osaka, Osaka 565-0871, Japan.

[6]Department of Virology and Immunology, Graduate School of Medicine, The University of Osaka, Osaka 565-0871, Japan.

[7]Laboratory of Translational Cancer Immunology and Biology, Next-generation Precision Medicine Research Center, Osaka International Cancer Institute, Osaka, Japan.

[#]These authors contributed equally to this work

Running title: Safety and efficacy of SA-5 in non-human primates

[*]**Corresponding author**:

Takuya Yamamoto

Laboratory of Precision Immunology, Center for Intractable Diseases and
ImmunoGenomics, National Institutes of Biomedical Innovation, Health and Nutrition,
Osaka 567-0085, Japan.
Tel:
yamamotot2@nibn.go.jp

Conflict of Interest

Mami Kochi, Shoko Ochiai, Hidenori Kimura, and Akihisa Fukushima are employees of Sumitomo Pharma Co., Ltd., Osaka, Japan. The SA-5 used in this study was provided by Sumitomo Pharma Co., Ltd. All other authors have declared that no conflict of interest exists.

Abstract

Toll-like receptor 7 (TLR7) agonists are promising immunostimulatory agents for the treatment of chronic infections and cancer. However, their systemic toxicity remains a challenge. In this study, SA-5, a novel liver-targeted, orally available TLR7 agonist, was evaluated for pharmacokinetics, safety, and efficacy in young and aged macaques across 1–10 mg/kg repeated doses. Safety was evaluated through hematologic, biochemical, and flow cytometric profiling, while efficacy was assessed via interferon (IFN)-α production, gene expression of interferon-stimulated genes, and plasmacytoid dendritic cell activation. A principal component analysis (PCA)-based composite scoring system was used to integrate multimodal parameters. SA-5 induced dose-dependent type I IFN with limited systemic inflammation, with 3 mg/kg showing optimal balance. SA-5 had comparable immunostimulatory activity to GS-9620 but with reduced adverse biomarker shifts. In aged macaques, efficacy was maintained with modestly increased safety responses. These findings support SA-5 as a safer next-generation TLR7 agonist effective across age groups, highlighting integrated biomarker profiling in preclinical immunomodulatory drug development.

Keywords

Non-human primates, innate immunity, TLR ligands, cynomolgus macaques, aging, immunosenescence.

Introduction

Pattern recognition receptors (PRRs), including toll-like receptors (TLRs), play a central role in sensing pathogens and initiating innate immune responses (1, 2) [1,2]. Among the TLRs, TLR7 is localized to intracellular compartments. It recognizes viral single-stranded RNA (ssRNA), leading to the induction of type I interferons such as IFN-α and IFN-β (3, 4) [3,4]. Given these functions, TLR7 has attracted attention as a potential therapeutic target for chronic viral infections and cancers.

Accordingly, the development of TLR7 agonists has been actively pursued with the aim of inducing type I interferons. For example, TLR7 ligands have been developed as therapeutic agents for chronic persistent infections such as AIDS and hepatitis B and C. In non-human primate models, particularly in the context of HIV-1 infection, TLR7 agonists have been designed to activate latently infected cells. Their use, either as a monotherapy or in combination with neutralizing antibodies, has been reported to exert therapeutic effects (5-7) [5-7]. A Phase Ib clinical trial was conducted in patients receiving combination antiretroviral therapy (cART), in which TLR7 agonists reduced proviral load and delayed viral rebound after treatment interruption. However, it was also

suggested that the administration of agonists increased the crosstalk between dendritic cells and natural killer (NK) cells, potentially enhancing cytotoxic activity (5) [5].

Similarly, preclinical non-human primate models of hepatitis B demonstrated the potential for a functional cure using TLR7 agonists due to their anti-HBV activity (8-10) [8-10]. However, a human single-dose study of GS-9620 (0.3–12 mg) in healthy volunteers showed systemic type I interferon induction, especially at higher doses (8–12 mg), alongside flu-like symptoms and lymphopenia, highlighting safety concerns (11) [11]. Subsequent clinical trials in patients with hepatitis B using lower GS-9620 monotherapy doses (0.3–4 mg, single or multiple) reported mild to moderate adverse events in 58% of participants (12) [12]. A phase II trial further indicated systemic type I interferon induction in approximately half of 21 patients, with a similar proportion experiencing flu-like symptoms, reinforcing concerns about the drug's safety profile (13) [13].

Consequently, the comprehensive evaluation of safety and efficacy is crucial for developing TLR7 agonists into potent immunostimulatory therapeutics. This requires

models that faithfully represent human physiology and enable accurate assessment of human TLR7 responses. Non-human primates (NHPs) are highly valuable preclinical models for TLR-targeting agent development due to their closer resemblance to human physiology, disease susceptibility, and TLR expression patterns compared to rodents (14) [14]. Furthermore, the greater genetic diversity within NHP populations, unlike genetically uniform mouse models, allows for the analysis of inter-individual variability in drug responses (15) [15].

In the present study, we utilized cynomolgus monkeys as an NHP model to evaluate the safety and efficacy of SA-5, a novel liver-targeted TLR7 agonist currently in clinical development by our group (16) [16]. Similar to GS-9620, SA-5 is an orally administered analog of the pyrimidine derivative DSP-0509 (17-19) [17-19]. SA-5 was specifically designed as a substrate for the organic anion-transporting polypeptides OATP1B1 and OATP1B3, which are expressed on hepatocyte sinusoidal membranes. Following oral administration, the compound travels through the intestinal tract and achieves high liver concentrations via the portal vein (16) [16]. Our investigation included assessing the pharmacokinetics (PK) and cytokine-inducing capacity of SA-5 after a single dose.

Furthermore, we conducted preclinical studies to evaluate SA-5's safety and efficacy under repeated dosing. Utilizing time-course samples from these repeated administrations, we performed a comprehensive, integrated analysis of multiple parameters—including hematologic and biochemical tests, ELISA-measured cytokine levels, and immune cell profiling via high-parameter flow cytometry—to create a single composite index for evaluating both safety and efficacy. Based on this composite index, we also performed a direct comparison with the reference compound GS-9620 and assessed age-dependent effects using aged cynomolgus monkeys.

Results

Single and Repeated Dose-Setting Study and Pharmacokinetics of the Oral TLR7 Ligand SA-5 in Monkeys

In this study, first, we conducted a single-dose pharmacokinetic (PK) study and cytokine analysis of the oral TLR7 ligand SA-5 (Figure 1A) in cynomolgus monkeys (Cohort 1, Figure S1A). The plasma concentration of SA-5 increased after its oral administration. In both sexes, the time to reach the maximum plasma concentration (T_{max}) was 6–8 h for all dose groups, except the 300 mg/kg group (Figure S2A, Table S1). The plasma exposure of SA-5, assessed by area under the plasma concentration-time curve (AUC_{0-t}) and maximum plasma concentration (C_{max}), increased in a dose-dependent manner (Table S1). In all dose groups, a clear induction of type I interferon (IFN)-α, interleukin (IL)-6, and IP-10 was observed, peaking at 6–8 h post-dosing. Tumor necrosis factor (TNF)- α was detectable only in the groups receiving 300 mg/kg or higher, and low levels were detected in the groups receiving 100 mg/kg or lower.

Furthermore, pharmacokinetic and repeated-dose toxicity studies were conducted in cynomolgus monkeys. These animals received once-weekly oral dosing for four

consecutive weeks, and plasma concentrations were measured at 2, 4, 8, 24, and 48 h after dosing in both the first and fourth weeks (Cohort 2, Figure S1A). Consistent with Cohort 1 findings, plasma SA-5 concentrations increased after oral administration. In the 10–100 mg/kg group, T_{max} was 8 h (Day 1 in Figure S2C and Table S2). Plasma exposure, assessed by AUC_{0-t} and C_{max}, showed a dose-dependent increase (Table S2 and Figure S2C). Notably, no clear correlation was observed between the C_{max} values of the first and fourth doses (Figure S2D). Comparison of AUC values indicated that the 10 mg/kg and 30 mg/kg groups were exposed to similar levels of SA-5 (Table S1 and Table S2). In the 30 mg/kg group, a clear induction of type I IFN was observed immediately after administration, suggesting that a similar response may also occur in the 10 mg/kg group. Furthermore, good tolerability up to 1000 mg/kg was confirmed with repeated administration for at least five weeks. Based on these results, a dosing regimen with a maximum dose of 10 mg/kg was adopted for the subsequent 12-week repeated administration study (Cohort 3, Figure S1A).

Safety Profile of the Oral TLR7 Ligand SA-5

Subsequently, the safety of repeated SA-5 administration at doses ≤10 mg/kg was evaluated (Cohort 3, Figure S1A). Six cynomolgus monkeys received oral SA-5 (1, 3, 5, or 10 mg/kg) every other week for 12 weeks, with blood sampling before dosing, 1 day post-dosing, and 7 days post-dosing (prior to the next administration); plasma and peripheral blood mononuclear cells (PBMCs) were isolated for subsequent analyses. To reduce sampling burden, only drug administration occurred at weeks 5, 6, 9, and 10.

Throughout the study, no notable changes in body weight were observed (Figure S3). Hematologic parameters were monitored after each SA-5 dose to evaluate drug-related changes (Figure. 1B and Figure S4), using statistical analyses comparing post-dosing values to both the first dosing day (Ad.0_d0) and the respective dosing day for each administration. The first administration showed a marked decrease in peripheral blood lymphocyte counts at ≥3 mg/kg one day post-dosing (Figure S4). However, from the second administration onward, no significant changes were detected at ≤3 mg/kg. At 5 and 10 mg/kg, considerable decreases were observed after the 12th and 7th administrations, respectively, but resolved within one week. Leukocyte subset analysis indicated a trend toward decreased lymphocyte and increased neutrophil fractions one

day post-administration without consistent statistical significance across dose groups (Figure 1B and Figure S4B). Other hematologic parameters showed no notable adverse effects (Figure S4C and S4D).

Biochemical inflammatory markers, analyzed similarly, revealed a dose-dependent elevation in C-reactive protein (CRP), with trend-level transient increases one day post-administration across all dose groups (q = 0.059-0.083), returning to baseline within one week (Figure 1C). Liver injury markers (aspartate aminotransferase [AST] and lactate dehydrogenase [LDH]) were markedly elevated one day post-administration across all dose groups (1–10 mg/kg) but returned to pre-dosing levels by one week (Figure 1D and Figure S5A). Comparisons between the first administration and values seven days after subsequent administrations showed no significant differences, suggesting no irreversible effects (Figure S5A). A positive correlation between AST and LDH and a partial correlation between AST and CRP were observed at doses ≥3 mg/kg one day post-administration (Figure S5B). While other parameters showed transient elevations, these were within expected inflammatory response ranges (Figure S5C and S5D). Minor, transient deviations in some liver function and inflammatory markers were noted

190 immediately post-dosing but subsided and returned to normal. Other biochemical
191 parameters showed no notable adverse effects (Figure S5C and S5D).
192
193 Plasma levels of pro-inflammatory cytokines IL-6 and TNF showed induction in some
194 high-dose individuals (5 and 10 mg/kg) one day post-administration, but no statistically
195 significant changes across dose groups (Figure S6A). Similarly, PBMC IL-6 and TNF
196 expression by reverse transcription polymerase chain reaction (RT-PCR) showed no
197 clear dose-dependent increase (Figure S6B), indicating no systemic inflammatory
198 cytokine induction up to 10 mg/kg.
199
200 High-parameter flow cytometry of PBMCs assessed SA-5's impact on cell frequency
201 and phenotype, focusing on monocytes. Intermediate monocytes (iMo; $CD14^{+}CD16^{+}$),
202 associated with inflammation and antigen presentation, showed a transient increase one
203 day post-dosing, returning to baseline by day 7 (Figure 1E and Figure S7A, S7B).
204 Notable iMo increases occurred at ≥3 mg/kg after the first dose (Figure 1E). Activation
205 markers CD80, CCR7, and CD169/Siglec-1 on iMos increased one day post-dosing and
206 returned to baseline by day 7 (Figure 1F and Figure S7D). Classical and non-classical

monocyte subsets were also analyzed (Figure S7). While frequency changes were most prominent and consistent in iMo, dose-dependent increases in activation markers at day 1 were detectable across all three subsets. This indicates that iMo provide the most sensitive marker of SA-5-induced myeloid activation, as they combine both expansion in frequency and upregulation of activation markers. Upon comparing the initial and final time points, a marked iMo increase was observed in the 5 mg/kg group, but no changes in activation marker expression were noted at any dose (Figure 1G and 1H).

Collectively, the transient changes in monocyte composition and iMo activation following SA-5 administration suggest a transient inflammatory response, consistent with hematologic and biochemical findings. Importantly, no statistically significant differences were observed between the initial and final dosing time points for any evaluated parameter, indicating that the observed safety-related changes during the 12 repeated administrations were transient.

Evaluation of Safety-Related Biomarkers

Next, to identify potential safety biomarkers, we integrated data from various analyses, comprehensively evaluating drug-induced responses, repeated dosing effects on baseline levels, and deviations from reference values by performing a group-wise comparison between low-dose (1–3 mg/kg) and high-dose (5–10 mg/kg) groups to extract parameters exhibiting dose-dependent changes (Figure 2A). Parameter extraction relied on three indices: (1) fold-change (FC) between pre-dosing and 1 d post-first administration, (2) FC between pre-dosing and 7 days after the 12th and final administration, and (3) a deviation score reflecting the extent of deviation from the established reference values (Figure S8).

For hematologic and biochemical parameters, a deviation scoring system was applied to 35 parameters with established reference ranges. The range unit was defined as the midpoint between the upper and lower reference limits. Deviations were categorized and scored: minor deviation (within the reference range limits = score 1), moderate deviation (exceeding the reference range by ≥1 range unit = score 2), and marked deviation (exceeding the reference range by ≥2 range units = score 4), with separate scores for deviations above and below the range (Figure S8). Calculating the difference

240 in deviation scores (delta scores) revealed a trend toward a dose-dependent increase
241 (Figure S8B, S8C).
242
243 Out of 132 parameters, 27 were identified as reflecting dose-responsive changes: 20
244 were associated with responses after the first administration, 3 reflected fold changes
245 after the final administration, and 4 were derived from the deviation score index (Figure
246 S9). For these selected parameters, we extracted: (1) FC between pre-dose and 1-day
247 post-dose for each administration, (2) FC relative to the baseline value prior to the first
248 administration across all dosing points, and (3) deviation scores from reference values.
249 These data were subjected to principal component analysis (PCA) to generate datasets
250 for each individual at each dosing point. PCA plotting of post-dosing day 1 (d1) values
251 for each administration (N = 6 animals × 4 dosing points = 24 data points) showed a
252 dose-dependent expansion in distribution (circle size), with PC1 shifting positively and
253 PC2 shifting negatively with increasing dose (Figure 2B). Based on probabilistic ellipse
254 areas, a dose-dependent expansion in distribution was observed (Figure 2C), suggesting
255 increasing inter-individual variability in off-target responses with dose, plateauing at 5
256 mg/kg. To assess repeated dosing effects, PCA plots were generated for the 1st, 2nd,

7th, and 12th administrations. In animals receiving ≥5 mg/kg, the 90% probabilistic ellipses after the 1st and 2nd doses were markedly shifted negatively, indicating the potential induction of qualitatively distinct off-target responses compared to ≤3 mg/kg (Figure 2D).

Evaluation of the Efficacy Profile of SA-5, an Oral TLR7 Agonist

Next, we investigated the induction of plasma type I IFN production, a key efficacy-related outcome of SA-5, resulting from its target TLR7 activation. Enzyme-linked immunosorbent assay (ELISA) measurement of plasma IFN-α levels post-SA-5 administration showed a consistent increase one day after dosing across all time points, exhibiting a clear dose-dependent trend (Figure 3A and Figure S10A). At 1 and 3 mg/kg, one monkey in each group showed no detectable IFN response, corresponding to no statistical significance at 1 mg/kg and a trend at 3 mg/kg (q = 0.079). Conversely, at 5 and 10 mg/kg, all animals displayed a robust IFN-α response after the first and second administrations, showing trend-level increases (q = 0.063) after multiple comparison correction. However, repeated dosing led to a gradual attenuation of this response over

time. Furthermore, comparing baseline and seven days post-final administration revealed no statistically significant differences at any dose (Figure 3B).

To further support these findings, quantitative RT-PCR in PBMCs examined type I IFN and interferon-stimulated gene (ISG) expression. Significant upregulation of ISGs IFIT1 and ISG15 occurred one day post-first administration across all dose groups (Figure 3C and Figure S10B). Notably, in the 5 mg/kg group, this upregulation was consistently observed one day after each administration (Figure S10B). While the 5 mg/kg group had the strongest gene induction after both the 1st and 12th administrations, the 10 mg/kg group showed weaker ISG upregulation than the 5 mg/kg group one day after the initial dose, suggesting potential suppression at excessive dosing. Comparing gene expression between the first administration and seven days post-final administration showed a marked increase at 3 and 5 mg/kg (Figure 3D).

Furthermore, we evaluated the abundance and activation of plasmacytoid dendritic cells (pDCs), which are known to highly express TLR7, a target of SA-5, major type I IFN sources, using high-parameter flow cytometry. A marked increase in pDC frequency

and activation marker CD80 expression was observed one day post-first administration at all doses, with a clear dose-dependent magnitude (Figure 3E, 3F, and Figure S10D). pDC activation decreased with repeated 5 and 10 mg/kg doses. After the 12th dose, considerable activation (MFI) was only observed at 10 mg/kg (Figure S10E), while frequency-based significance was only noted at 3 mg/kg. Myeloid dendritic cells (mDCs) showed similar activation patterns to pDCs, with no significant activation at 1 mg/kg after the first dose but clear activation at ≥3 mg/kg.

Comparing the first administration and seven days post-final administration revealed no statistically significant changes in pDCs or mDCs at any dose (Figure 3G and 3H). Analyzing the relationship between plasma IFN-α and ISG expression one day post-administration showed no significant correlation for *IFIT1* or *ISG15* (Figure S10C), suggesting their potential as independent biomarkers of type I IFN pathway activation. In contrast, a strong positive correlation was observed between plasma IFN-α and pDC activation at doses ≥3 mg/kg (Figure 3I).

Evaluation of Efficacy-Related Biomarkers

Finally, to identify efficacy-related biomarkers, we integrated data from various analyses, selecting nine markers associated with type I IFN-α induction: plasma IFN-α levels, expression of seven interferon-stimulated genes (ISGs) in PBMCs via qRT-PCR, and the frequency of activation markers on pDCs, the primary type I IFN source. These markers underwent PCA for comprehensive evaluation (Figure 4A). The PCA revealed a dose-dependent shift, with PC1 increasing positively and PC2 shifting negatively (Figure 4B). The 90% probabilistic ellipse area decreased dose-dependently, indicating convergence toward a distinct phenotypic pattern at higher doses (Figure 4C). Separate PCA plots for the 1st, 2nd, 7th, and 12th administrations showed 90% ellipse convergence after the 1st and 2nd doses at doses ≥3 mg/kg, while no such convergence occurred at 1 mg/kg across all time points. This suggests that efficacy-related immune activation occurred at doses of 3 mg/kg or higher (Figure 4D). Notably, the degree of convergence decreased after the 7th and 12th administrations. Collectively, these findings indicate that SA-5 has the potential to activate the type I IFN pathway when administered at ≥3 mg/kg for at least two doses.

Integrated Analysis of Safety and Efficacy

To evaluate the relationship between safety and efficacy in individual cynomolgus monkeys, we plotted the PC1 values obtained from the respective PCAs of safety (PC1-safety) and efficacy (PC1-efficacy) parameters (Figure 5A). This visualization revealed a dose-dependent upward-sloping distribution pattern.

Using the values at 1 mg/kg as a reference, statistical comparisons were performed for each PC1 axis. A significant increase in PC1-safety was observed one day after administration at doses of 5 and 10 mg/kg, indicating that safety was likely maintained at doses of up to 3 mg/kg (Figure 5B). In contrast, for efficacy, considerable differences were observed at doses of 3 mg/kg and above (Figure 5C).

To further assess the magnitude of individual responses in cynomolgus monkeys, we classified the animals into four groups based on PC1-safety and PC1-efficacy values, using the maximum value of the 1 mg/kg probabilistic ellipse as a threshold. The groups were defined as follows: low safety and low efficacy (G1_DN); high safety and low efficacy (G2_Safety); low safety and high efficacy (G3_Efficacy); and high safety and efficacy (G4_Both) (Figure 5D). This classification revealed that animals exhibiting

high efficacy (PC1-efficacy) began to appear at a dose of 3 mg/kg, whereas animals showing elevated safety responses (PC1-safety) were evident from 5 mg/kg onward (Figure 5E).

To validate the PCA results, we examined the dose dependency of representative parameters for safety and efficacy: CRP and IFN-α, respectively. Both markers showed a dose-dependent trend toward increased median values (Figure 5F and 5G). Furthermore, correlation analyses between the 1st and 12th administrations revealed a strong positive correlation for both CRP and IFN-α (Figure 5H and 5I), suggesting that the integrated analysis captured consistent trends across repeated dosing.

Based on these findings, a dose of 3 mg/kg was concluded to represent the optimal balance between safety and efficacy, as it demonstrated therapeutic activity while maintaining an acceptable safety profile.

Comparative Evaluation of the Predecessor TLR7 Ligand GS-9620 and SA-5

Next, a comparative analysis was conducted using the existing agent GS-9620. Body weights remained stable throughout the study period in both treatment groups (Figure S11A and S11B). Evaluation of serum CRP levels as a safety marker revealed no significant changes in the SA-5 group at 1 mg/kg. In contrast, the GS-9620 group exhibited remarkable increases at multiple time points (Figure 6A). In contrast, regarding IFN-α as an efficacy marker, the SA-5 group showed a trend toward induction one day after dosing, while the GS-9620 group demonstrated no clear induction ("blip") (Figure 6B).

Using the same PCA-based approach shown in Figure 5, we plotted the safety and efficacy responses for each group. Both groups exhibited notable shifts one day after dosing; however, while safety scores in the SA-5 group remained below the defined threshold, those in the GS-9620 group markedly exceeded this threshold (Figure 6C). Group-wise statistical comparisons revealed no significant difference in PC1-efficacy between the two groups. In contrast, PC1-safety was markedly elevated in the GS-9620 group one day after dosing, suggesting that SA-5 had a considerably better safety profile than GS-9620 (Figure 6D and 6E). Furthermore, using the classification method

described in Figure 5E, safety-efficacy profiling showed that approximately half of the animals in the GS-9620 group fell into categories associated with safety concerns (Figure 6F).

To validate the PCA results, representative safety and efficacy parameters—CRP and IFN-α—were compared between the two groups. While no significant difference in IFN-α levels was observed, serum CRP levels were notably higher in the GS-9620 group compared to the SA-5 group (Figure 6G and 6H). Additionally, the deviation score was markedly higher in the GS-9620 group (Figure S11C). Collectively, a comprehensive comparison at an equivalent dose level suggested a superior safety profile for SA-5.

Investigation in Aged NHPs

Finally, we conducted a comparative analysis at the 3 mg/kg dose—identified as both safe and effective—to evaluate age-related differences, focusing on an aged group (≥20 years old; Figure S12A). Except for one animal in the aged group, the body weight remained stable throughout the study period in both the young and aged groups (Figure

391 S12B, S12C). The evaluation of serum CRP levels as a safety marker revealed no
392 significant changes in the young group. In contrast, the aged group exhibited
393 remarkable increases at multiple time points (Figure 7A). Additionally, the deviation
394 score was considerably higher in the aged group (Figure S12D).
395
396 In contrast, for the efficacy marker IFN-a, both young and aged groups exhibited a trend
397 toward induction one day after dosing (Figure 7B). Using the PCA-based analysis
398 described in Figure 5, we plotted the safety and efficacy responses, which revealed clear
399 shifts one day after administration in both groups. Notably, the aged group exhibited a
400 positive directional shift along both axes (Figure 7C). Group-wise statistical
401 comparisons showed a significant increase in the aged group one day after dosing,
402 suggesting a modest increase in safety-related concerns. Simultaneously, efficacy was
403 maintained (Figure 7D and 7E). When the safety and efficacy classification was
404 performed using the framework described in Figure 5E, none of the individuals in either
405 group fell into the category associated with safety concerns alone. Furthermore,
406 approximately half of the animals in the aged group showed an efficacy profile (Figure
407 7F).

To validate the PCA results, representative safety and efficacy parameters—CRP and IFN-a—were compared between the young and aged groups. Both these parameters were markedly higher in the aged group (Figure 7G and 7H). Collectively, these findings from a comprehensive comparison at the same dose level suggest that although safety-related concerns may increase, SA-5 retains the potential to elicit efficacy even in aged individuals.

Discussion

TLR7 agonists are actively being developed as therapeutic agents for chronic persistent infections and cancer (20-23) [20-23]. In particular, their potential as treatments for chronic infections such as HBV and HIV, either as monotherapy or in combination with other therapeutic strategies, has been explored, and some candidates have already advanced to clinical trials in humans (5, 9, 12, 13, 24-26) [5,9,12,13,24-26]. However, to date, no TLR7 agonist has received regulatory approval for any indication, primarily due to safety or efficacy limitations. Therefore, the development of novel agents that can overcome the shortcomings of the existing compounds is critical.

In this study, we conducted preclinical evaluations of SA-5 in cynomolgus monkeys. Pharmacokinetic profiling of SA-5 was performed, and a comprehensive safety assessment was conducted by selecting dose-dependent parameters and applying an integrated analysis of multilayered datasets. Across the tested doses of 1, 3, 5, and 10 mg/kg, transient reductions in peripheral blood lymphocytes and increases in biochemical markers and inflammatory response indicators were observed, with most parameters returned to baseline within one week of administration. Among monocyte

subsets, iMo, which are involved in inflammatory cytokine production, showed the most pronounced and consistent changes. They exhibited dose-dependent increases in frequency and activation markers at day 1, with values generally resolving by day 7, except for a sustained elevation at 10 mg/kg. Classical and non-classical monocytes also displayed activation at day 1, albeit less prominently (Figure S7). Therefore, iMo represent the most sensitive readout of SA-5-induced myeloid activation. To assess safety from multiple perspectives, including short- and long-term effects, as well as deviations from reference values, we evaluated changes from baseline after 12 repeated doses, dose-by-dose fluctuations before and after administration, and deviation scores. PCA revealed a dose-dependent expansion of the probabilistic ellipses. Notably, after the first and second administrations, animals receiving ≥5 mg/kg showed distributions that were markedly different from those in the 3 mg/kg group, suggesting the possibility of qualitatively distinct off-target responses at higher doses.

In preliminary single-dose NOAEL studies, administration of SA-5 up to 1000 mg/kg appeared tolerable, although the very small cohort size (n=2 per group; Figure S1 and Figure S2) precluded robust statistical conclusions. On this basis, we set 10 mg/kg as

451 the upper limit for the repeated-dose evaluation, as it was the lowest dose at which
452 safety-related changes were initially noted in the PK study. In a 12-week repeated-dose
453 study with larger cohorts (n=6/group, 1–10 mg/kg), safety deviations—including CRP
454 elevation (Figure 1C and Figure S5A), dose-dependent expansion of the safety PCA
455 distribution (Figure 2B–D), and intermediate monocyte alterations (Figure 1F, G and
456 Figure S7)—emerged at ≥5 mg/kg, whereas clear efficacy, evidenced by IFN-α
457 induction and pDC activation (Figure 3I), was already detectable at 3 mg/kg.
458 Accordingly, integrated analysis demonstrated that 3 mg/kg represented the optimal
459 balance between safety and efficacy. Importantly, in aged macaques, CRP elevations
460 were observed even at 3 mg/kg, highlighting the need for careful monitoring in older
461 populations. While these findings led us to select 3 mg/kg as the recommended dose for
462 further pursuit, the more favorable safety profile of SA-5 compared with GS-9620
463 suggests that exploration of higher doses (>5 mg/kg) may still be feasible in future
464 studies.

465

466 Extensive preclinical and clinical data have been accumulated on GS-9620, a previously
467 developed TLR7 agonist. In human studies, GS-9620 was administered at doses ranging

468 from 1 to 12 mg in healthy individuals, as well as in patients with HBV or HIV
469 infection. Most adverse events were classified as grade 1 or 2, and the drug was
470 considered safe at lower doses (11, 13) [11,13]. However, in a Phase I study conducted on
471 healthy volunteers, adverse events, including flu-like symptoms, were observed in
472 88.3% and 100% of the participants receiving 8 mg and 12 mg, respectively, leading to
473 a recommendation for low-dose administration (11) [11]. The inability to administer
474 higher doses owing to adverse effects is a major limitation of GS-9620.
475
476 For the efficacy assessment, we focused on type I IFN, a key mediator of the antiviral
477 immune response against infected cells. Although one non-responder was observed in
478 both the 1 and 3 mg/kg SA-5 groups, a dose-dependent increase in circulating type I
479 IFN levels was observed, indicating the immunostimulatory potential of SA-5.
480 Supporting its clinical potential, a recent study using an HBV-infected mouse model
481 demonstrated that the administration of SA-5 at 3 mg/kg markedly induced ISG15
482 through type I IFN signaling, resulting in a marked reduction in HBV DNA levels (16)
483 [16]. In contrast, although GS-9620 has been shown to induce both type I IFN secretion
484 and ISG15 expression in HBV-infected patients, it ultimately failed to achieve a

485 significant reduction in HBsAg levels and thus did not progress to clinical application
486 (11) [11]. One of the limitations that may have contributed to the lack of clinical efficacy
487 of GS-9620 is the inability to administer high doses due to adverse effects. In a Phase I
488 study involving healthy volunteers, plasma drug levels at doses ≤4 mg were markedly
489 lower than those observed at 8–12 mg, suggesting that clinical trials conducted at ≤4 mg
490 in patients with chronic HBV may not have achieved sufficient therapeutic exposure
491 (11-13, 24) [11-13,24]. These findings highlight the importance of identifying agents or
492 dosing regimens that allow the highest possible exposure while minimizing off-target
493 responses. In the case of SA-5, careful evaluation of the efficacy in human subjects is
494 required. Notably, the induction of circulating type I IFN declined with repeated dosing
495 at all dose levels. A similar trend was observed for the activation of pDCs, the primary
496 producers of type I IFN (27, 28) [27,28], which diminished over the course of repeated
497 administration. This suggests that pDC desensitization contributes to the attenuation of
498 IFN responses (28) [28]. Although frequency-based analyses at 3 mg/kg did not reach
499 statistical significance, median values and CD80 MFI indicated activation consistent
500 with IFN-α induction.

In addition, myeloid dendritic cells displayed activation patterns broadly similar to pDCs, with significant CD80 upregulation at ≥3 mg/kg (Figure S10), indicating that SA-5 engages multiple antigen-presenting cell subsets with distinct magnitudes and kinetics.

However, it should be noted that the efficacy assessment in this study was limited to an indirect evaluation based on type I IFN pathway activation. As with GS-9620, direct confirmation of the clinical efficacy of SA-5 in humans is required.

Although the present study primarily focused on the safety and efficacy of SA-5, its adjuvant activity is likely mediated through TLR7 activation. This assumption is supported by structural similarity to DSP-0509, a validated TLR7 agonist, and by our own data showing concentration-dependent activation of recombinant human and cynomolgus TLR7-expressing cells, as well as functional activation of pDCs, the principal $TLR7^+$ population in these species. Through this pathway, SA-5 induces type I IFN responses, a key driver of its immunostimulatory effects. Future work, including in vivo pDC depletion studies or in vitro analyses using purified immune subsets, will be valuable to more precisely delineate this mechanism. Furthermore, in comparison with

GS-9620, the targeted distribution of SA-5 may favor localized pDC activation, which could contribute to reduced systemic adverse effects.

Based on our findings, we propose 3 mg/kg as the recommended dose of SA-5 to achieve a favorable balance between safety and efficacy. When comparing SA-5 and the existing TLR7 ligand GS-9620 at an equivalent dose of 1 mg/kg, SA-5 exhibited comparable efficacy, whereas GS-9620 was associated with markedly lower safety. SA-5 is designed for intestinal-specific delivery, allowing hepatic targeting via the portal vein and subsequent biliary excretion (16) [16]. This delivery mechanism likely contributes to reduced systemic exposure, which may underlie the superior safety profile of SA-5 compared to that of GS-9620 observed in our comparative study. Indeed, in a clinical trial involving 192 patients with HBV who had not received prior antiviral therapy, 65.9% experienced adverse events during 24 weeks of GS-9620 administration (24) [24]. The most common symptoms are flu-like manifestations, such as fever and myalgia, raising concerns about systemic effects. Among patients receiving 1, 2, or 4 mg doses, grade 3 adverse events, such as elevated liver enzymes and flu-like symptoms, led to treatment discontinuation in 2 patients (3.6%) at 2 mg and 4 patients

534 (7.9%) at 4 mg. In the present study, although SA-5 demonstrated efficacy comparable
535 to that of GS-9620, it was associated with lower CRP levels and fewer adverse
536 responses, suggesting a reduction in systemic immune activation. Notably, SA-5
537 showed a comparable safety profile at both 1 and 3 mg/kg, indicating its potential for
538 higher dosing with reduced systemic toxicity compared to GS-9620. These results
539 suggest that SA-5 may overcome one of the primary limitations of GS-9620, namely,
540 the inability to administer therapeutically effective high doses owing to adverse effects.
541
542 However, given that many patients with potential target indications for SA-5, such as
543 chronic persistent infections and cancer, are middle-aged or older, it is essential to
544 evaluate age-related changes in efficacy and risk (29) [29]. Therefore, the assessment of
545 SA-5 should include safety and efficacy evaluations using appropriate aging models that
546 account for physiological aging. Among the experimental animals, non-human primates
547 are generally considered the most physiologically relevant to humans because of their
548 close genetic similarity (30) [30]. We previously demonstrated that genes identified
549 through gene expression profiling of liver tissues from both young and aged
550 cynomolgus monkeys were markedly upregulated in aged human liver samples,

551 supporting the relevance of cynomolgus monkeys as a useful model for studying liver
552 aging (31) [31]. In addition, we have previously evaluated the safety and efficacy of
553 STING ligands, another class of innate immune activators, in both young and aged
554 cynomolgus monkeys (15) [15]. In the study, aged monkeys exhibited reduced safety and
555 efficacy compared to younger animals, and an inverse correlation was observed between
556 age and both type I IFN induction and pDC activation. In contrast, in the present study,
557 although aged monkeys exhibited a decrease in safety compared with younger animals,
558 an increase in efficacy was observed. Among individual animals, we identified subsets
559 showing improved efficacy without changes in safety, as well as those with increased
560 efficacy accompanied by decreased safety. However, no individuals were observed in
561 whom safety declined without a corresponding increase in efficacy.

562 Regarding potential sex-related differences, although the number of animals analyzed
563 was small and does not allow firm conclusions, our supplemental data (Figure S2)
564 suggest that female monkeys may exhibit higher baseline levels of SA-5 compared with
565 males. This observation warrants further investigation in future studies with larger
566 cohorts.

In vitro studies using DCs isolated from the PBMCs of aged and young individuals have reported that stimulation with the TLR7/8 ligand R848 results in reduced type I IFN production in aged donors. These studies also demonstrated decreased expression of TLR7 in pDCs derived from aged individuals (32, 33) [32,33]. In contrast, in the present in viv*o* dosing study, both type I IFN gene expression and secretion were elevated in PBMCs from aged cynomolgus monkeys, indicating a different response profile compared to previous reports. These discrepancies underscore the importance of cautious evaluation when considering drug administration in the older population. Six animals were used per group. Given this sample size, the presence of even a single non-responder can obscure statistically significant differences; conversely, a strong response in one animal may produce apparent but non-significant trends. Therefore, the conclusions drawn from comparisons that did not reach statistical significance should be interpreted with caution.

In conclusion, we evaluated the efficacy and safety of SA-5, a novel TLR7 ligand, in a non-human primate model. Our findings suggest that SA-5 may offer a safer dosing

584 profile than the existing oral TLR7 agonist GS-9620. Importantly, the methodological
585 framework established in this study is expected to serve not only in the clinical
586 development of SA-5 but also as a valuable approach for determining appropriate dose
587 settings in future first-in-human trials of similar innate immune stimulators.
588 This study highlights the potential of SA-5 as a novel TLR7 agonist with an improved
589 safety profile over GS-9620, supported by integrated analyses combining
590 pharmacokinetics, safety biomarkers, and type I IFN-related efficacy parameters. These
591 findings not only demonstrate the feasibility of hepatic-targeted TLR7 activation but
592 also establish a methodological framework for balanced dose selection in the preclinical
593 setting. Notably, the identification of a 3 mg/kg dose as optimal suggests a potential
594 translational window for future human studies.
595

596 For future research, several directions should be pursued. First, mechanistic studies are
597 needed to elucidate the molecular basis of the attenuated type I IFN response observed
598 with repeated dosing, including the potential desensitization of plasmacytoid dendritic
599 cells. Second, since aged animals exhibited distinct immunological responses to SA-5,
600 further investigation into age-associated modulation of innate immunity could refine

patient stratification and dosing strategies. Third, while this study focused primarily on innate immune responses, we also evaluated T-cell activation markers such as CD69 on $CD4^+$ and $CD8^+$ T cells. These results were inconsistent and did not show a clear dose-dependent pattern (data not shown), so no reliable conclusions could be drawn regarding T-cell activation under the present conditions. Nevertheless, murine studies have reported SA-5-induced T-cell activation, suggesting that species-specific factors or methodological limitations may explain the discrepancy. Further optimization of experimental conditions may therefore be required to clarify whether SA-5 can also induce adaptive T-cell responses in primates. Finally, clinical studies will be essential to determine whether the safety-efficacy balance observed in NHPs translates to humans, particularly in populations with chronic viral infections or cancer. The composite biomarker and PCA-based analytical strategy presented here may also be applicable for early-stage clinical decision-making in the development of innate immune modulators.

615 **Methods**

616 ***Sex as a Biological Variable***

617 Our study examined male and female animals, and similar findings are reported for
618 both sexes for cohort 1 and 2. However, owing to the limited sample size, sex-stratified
619 analyses were not performed.

620 ***Animal Experiments, PBMC Sampling, and Hematologic Analysis***

621 For cohort 1, eight cynomolgus macaques (4 males and 4 females, 2–3 years of age)
622 were randomly assigned to four groups (n = 1 male and 1 female per group). Each
623 animal received a single oral dose of SA-5 at 30 mg/kg, 100 mg/kg, 300 mg/kg, or 1000
624 mg/kg.

625 For cohort 2, sixteen cynomolgus macaques (8 males and 8 females, 2–3 years of age)
626 were randomly assigned to four groups (n = 2 males and 2 females per group). Animals
627 received SA-5 at doses of 0 mg/kg (vehicle control: 0.5% w/v methylcellulose solution),
628 10 mg/kg, 100 mg/kg, or 1000 mg/kg. Dosing was performed once weekly for four
629 weeks, for a total of five administrations.

630 In these cohorts, blood samples were collected at 1, 2, 4, 6, 8, 24, 48, and 72 h post-
631 administration using syringes and needles pre-treated with dipotassium

ethylenediaminetetraacetic acid (EDTA-2K) for PK and cytokine analyses. Plasma was separated from whole blood and promptly frozen, then stored in an ultra-low temperature freezer until analysis.

Plasma concentrations of SA-5 were determined using a liquid chromatography–tandem mass spectrometry (LC-MS/MS). Plasma samples were prepared by protein precipitation and injected into the LC-MS/MS. The pharmacokinetic parameters such as C_{max}, T_{max}, and AUC_{0-t} were obtained using non-compartmental analysis with Phoenix WinNonlin software (version 6.4; Certara INC., Radnor, PA, USA). Cytokine levels were measured using electrochemiluminescence (ECL) and Luminex-based assays. IP-10, TNF-α, and IL-6 were quantified using the U-PLEX Biomarker Group 1 (NHP) kit (Meso Scale Diagnostics, LLC., Rockville, MD, USA), while IFN-α was measured using the IFN-alpha Monkey ProcartaPlex Simplex kit (Thermo Fisher Scientific Inc., Waltham, MA, USA).

For cohort 3, Thirty-six cynomolgus macaques aged 4–20 years were divided into six groups (1 mg/kg (n=6), 3 mg/kg (young n=6, aged n=6), 5 mg/kg (n=6), and 10 mg/kg (n=6) for SA-5, and 1 mg/kg (n=6) for GS-9620; Table S3). Macaques were orally administered increasing doses of either SA-5 or GS-9620 at 1-week intervals.

649

650 PBMCs and plasma were isolated from blood samples collected at each time point in
651 tubes containing EDTA using Ficoll-Paque PLUS (GE Healthcare, Buckinghamshire,
652 UK). Purified PBMCs were incubated in fetal bovine serum (FBS; Sigma-Aldrich, St.
653 Louis, MO, USA) containing 10% DMSO (Sigma-Aldrich, St. Louis, MO, USA,
654 hereafter Sigma) and stored in liquid nitrogen until analysis. Complete blood counts
655 were performed using freshly isolated blood using an automated hematology analyzer
656 (Sysmex K-4500; Sysmex, Hyogo, Japan).

657

658 ***ELISA Assay***

659 For cohort 3, plasma was obtained from the blood supernatant during PBMC
660 purification and cryopreserved until further use. Plasma cytokine levels were analyzed
661 using ELISA kits purchased from MABTECH (Nacka Strand, Sweden) for evaluating
662 human IL-6 (3460-1H-6), human IFN-α (3425-1H-6), and monkey TNF (3512M-1H-6)
663 according to the manufacturer's protocol. The ELISA signals were detected using an
664 Epoch 2 Microplate Spectrophotometer (BioTek).

665

qRT-PCR

mRNA was extracted from PBMCs using an RNeasy Mini Kit from PBMC (Qiagen, Hilden, Germany). To synthesize cDNA, isolated mRNA was reverse-transcribed using the SuperScript^{TM} III First-Stand Synthesis System (Invitrogen). qRT-PCR was performed using HUNDERBIRD Probe qPCR Mix (TOYOBO, Japan), RT enzyme (Invitrogen, Thermo Fisher Scientific), ROX (Invitrogen, Thermo Fisher Scientific), TaqMan probes for candidate genes (CCL3, Rh02788104_gH; CXCL11, Rh02621763_m1; Eukaryotic 18S rRNA_ Hs99999901_s1; IFIT1, Rh00929909_m1; IFNA1, Hs 00256882_s1; IFNB1, Rh02913347_s1; IL1B, Rh02621711_m1; IL6, Rh02621719_u1; IL23A, Rh02872166_m1; IRF7, Rh02839174_m1; ISG15, Rh02915441_g1; MX1, Rh02842279_m1; TNF, Rh02789784_m1), and a reference gene (GAPDH, Forward, 5′-AGAAGTATACAACAGCCTCA-3′; Reverse, 5′-ACTGTGGTCATGAGTCCTTC-3′; FAM, 5′-ACCACCAACTGCTTAGCACC-3′), with StepOne Plus Real-time PCR system. The following thermal cycling conditions were used: 30 min at 45 °C, 5 min at 95 °C, 40 cycles of 1 s at 95 °C, 30 s at 54 °C, and 30 s at 60 °C for MX1, and CXCL11, 40 cycles of 1 s at 95 °C, and 60 s at 60 °C for others.

683

684 ***Flow Cytometric Analysis***

685 Frozen PBMCs were thawed and washed with Roswell Park Memorial Institute 1640
686 medium (Sigma) supplemented with 10% FBS (Sigma), 100 unit/mL penicillin, and 100
687 mg/mL streptomycin (Sigma, the supplemented medium hereafter R10). The cells were
688 treated with 1 mL of 50 U/mL benzonase (Merck, Darmstadt, Germany) in R10 for 60
689 min at 37 °C. After incubation, the cells were stained using a Fixable Viability Stain
690 440UV kit (FVS440; Becton, Dickinson, and Co. Franklin Lakes, NJ, USA; BD) at
691 room temperature (hereafter RT) for 5 min at room temperature. The CC-chemokine
692 receptor 7 (CCR7) was stained at 37 °C for 10 min, and the antibodies for the remaining
693 markers listed in Table S4 were added and incubated at RT for 15 min. After staining,
694 cells were washed twice with PBS, fixed with 1% paraformaldehyde, and analyzed
695 using the FACSymphony A5SE flow cytometer (BD) equipped with 5 lasers.

696

697 ***Flow Cytometry Data Processing for Safety and Efficacy Evaluation of Individual***
698 ***Macaques***

FCS files were analyzed using FlowJo software (version 10.10.0; Becton, Dickinson, and Co., Franklin Lakes, NJ, USA). Plots were generated using R software version 4.1.0. by using the listed packages.

Multiparameter Analysis for Safety and Efficacy Evaluation of Individual Macaques

The experimentally obtained raw data were preprocessed as follows: First, a minimum threshold value was set; if the minimum value of a parameter was less than zero, the threshold was set to zero. For the fold-change calculation, if the baseline value was zero, the nearest nonzero value was extracted and used as the baseline value.

To align the post-administration time points (0, 1, and 7 days) for each administration, we selected four administration points: Ad.01, Ad.02, Ad.07, and Ad.12. Day 0 (d0) of the next administration was set to be the same as day 7 (d7) of the previous administration (e.g., d7 of Ad.01 and d0 of Ad.02 refer to the same data). The fold-change (FC) values were calculated relative to day 0 for each administration and day 0 for the first administration.

716 To score the outlier values in complete blood count and biochemical tests, we first
717 selected 35 parameters for which standard ranges were available. We calculated the
718 median value of each standard range and set two thresholds: tier 1 thresholds were
719 defined as the upper limit plus half of the median value and the lower limit minus half
720 of the median value, and tier 2 thresholds were defined as the upper limit plus the full
721 median value and the lower limit minus the full median value. If the actual value
722 exceeded the standard range, a score of +1 was assigned. If the score exceeded the Tier
723 1 threshold, a score of +2 was assigned. If it exceeded the Tier 2 threshold, a score of +4
724 was assigned. The total score was defined as the CBC score for outlier evaluation.
725 Consequently, the outlier levels were categorized as follows: 0, within range; 1 = weak
726 outlier; 3 = moderate outlier; and 7, strong outlier.
727
728 PCA was performed using the *prcomp* function in the R statistical package. The PCA
729 plots for safety and efficacy were generated separately using the selected parameters, as
730 schematically shown in Figure 2A and 4A, respectively. Briefly, for the safety PCA, the
731 parameters associated with dose-dependent differences were selected as follows: The
732 experimental groups were further divided into two groups based on the dose levels: 1–3

mg/kg and 5–10 mg/kg. The following parameters were compared: (1) actual values and fold-change values one day after the first administration (Ad.01d1/Ad.01d0), (2) fold-change values relative to the baseline value prior to the first administration across all dosing points, and (3) deviation scores from reference values. We compared the intergroup differences using the Wilcoxon test and extracted 27 parameters that showed statistically significant differences. For efficacy PCA, we manually selected 10 parameters known to be involved in type I IFN signaling.

To create a plot that simultaneously shows the analysis for safety and efficacy, PC1 values from the safety and efficacy PCA data were combined and plotted in a two-dimensional space. Individual macaques were classified into four groups based on PC1 values for safety and efficacy, with the threshold defined by the maximum value of the ellipse.

Statistical Analysis

Statistical analyses were performed using R/Bioconductor (R version 4.4.2) or GraphPad Prism software (version 8.3.0; GraphPad Software, San Diego, CA, USA).

The experimental variables were compared using the nonparametric Wilcoxon/Mann–Whitney *U* test unless otherwise stated. For analyses comparing dose groups across multiple administrations, the Wilcoxon rank-sum test stratified by administration (Van Elteren test) was used. When multiple comparisons were performed, p-values were adjusted using the Benjamini–Hochberg false discovery rate (FDR) method, and adjusted *q*-values were reported. Statistical significance was defined as $p < 0.05$ for single comparisons and FDR-adjusted $q < 0.05$ for analyses involving multiple comparisons, unless otherwise noted. For the cytokine correlation data, each cytokine concentration in the plasma was scaled, variances were adjusted to one within parameters using the *scale* function of the R scales package, and Spearman's correlation values were calculated.

Animals and Ethical Compliance for Animal Experiments

Cynomolgus macaques (Macaca fascicularis) used in Cohorts 1 and 2 were confirmed to be negative for simian immunodeficiency virus (SIV), simian type D retrovirus, simian T-cell leukemia virus, B virus, and filoviruses. All animals were bred at NAFOVANNY (Dong Nai, Vietnam) and supplied by Eve Bioscience (Wakayama,

767 Japan). Animal studies were performed at the SNBL INA Ltd. (Nagano, Japan), an
768 AAALAC International-accredited facility. All procedures were approved by the
769 Institutional Animal Care and Use Committee (IACUC) of SNBL INA Ltd. (Approval
770 No. 22066 for Cohort 1 and No. 22115 for Cohort 2). Animals were housed and
771 monitored under the supervision of the veterinarian. For cohort 3, cynomolgus
772 macaques, all of which were negative for SIV, simian type D retrovirus, simian T-cell
773 lymphotropic virus, simian foamy virus, Epstein–Barr virus, cytomegalovirus, and B
774 virus, housed at the Tsukuba Primate Research Center (TPRC), National Institutes of
775 Biomedical Innovation, Health, and Nutrition (NIBN), were used. Animal studies were
776 performed at NIBN with the approval of the institutional Committee on the Ethics of
777 Animal Experiments of NIBN (Approval #DSR03-22). The animals were supervised by
778 the veterinarians in charge of the animal facility.
779
780 **Data Availability Statement**
781 The data generated and/or analyzed in this study are available from the corresponding
782 author upon reasonable request. Values for all data points in graphs are reported in the
783 Supporting Data Values file.

784

50

Acknowledgments

We would like to thank Drs. Yasuhiro Yasutomi and Tomotaka Okamura at the Tsukuba Primate Research Center, National Institutes of Biomedical Innovation, Health, and Nutrition, for their valuable discussions and support. We thank the members of the Laboratory of Precision Immunology for their excellent technical support. We also thank HAMRI Co., Ltd. and the Corporation for Production and Research of Laboratory Primates for their support with animal experiments. This study was supported by the Japan Society for the Promotion of Science/Scientific Research (B) (Grant number: JP20H03728) and the Japan Agency for Medical Research and Development (Grant number: JP25fk0310542).

Author contributions

S.T.: Conceptualization, Methodology, Investigation, Formal analysis, Visualization, Writing – original draft, and funding acquisition.

T.T.: Investigation, Formal analysis, Visualization, Writing – original draft.

Y.N., H.M., T.N.: Investigation, Resources.

S.Y., T.K.: Supervision, Conceptualization, Writing – review & editing.

M.K., S.O., H.K., A.F.: Resources, Investigation (compound synthesis and pharmacokinetics).

T.Y.: Conceptualization, Supervision, Project administration, writing the original draft, writing the review and editing, and funding acquisition.

All authors: Writing – review & editing, Approval of final manuscript.

All authors read and approved the final manuscript.

S.T. and T.T. contributed equally to this work. Both authors were involved in the design, execution, and analysis of the experiments, and co-wrote the original draft. The order of authorship among co–first authors was determined based on the extent of their contributions to experimental design, data analysis, and manuscript preparation.

Declaration of interests

The authors declare no conflicts of interest, except that Mami Kochi, Shoko Ochiai, Hidenori Kimura, and Akihisa Fukushima are employees of Sumitomo Pharma Co., Ltd., Osaka, Japan. The SA-5 used in this study was provided by Sumitomo Pharma Co., Ltd.

819

820

References

1. Broz, P., and Monack, D.M. (2013). Newly described pattern recognition receptors team up against intracellular pathogens. Nat Rev Immunol *13*, 551–565. 10.1038/nri3479.

2. Cao, X. (2016). Self-regulation and cross-regulation of pattern-recognition receptor signalling in health and disease. Nat Rev Immunol *16*, 35–50. 10.1038/nri.2015.8.

3. Iwasaki, A., and Medzhitov, R. (2004). Toll-like receptor control of the adaptive immune responses. Nat Immunol *5*, 987–995. 10.1038/ni1112.

4. Akira, S., Uematsu, S., and Takeuchi, O. (2006). Pathogen recognition and innate immunity. Cell *124*, 783–801. 10.1016/j.cell.2006.02.015.

5. SenGupta, D., Brinson, C., DeJesus, E., Mills, A., Shalit, P., Guo, S., Cai, Y., Wallin, J.J., Zhang, L., Humeniuk, R., Begley, R., et al. (2021). The TLR7 agonist vesatolimod induced a modest delay in viral rebound in HIV controllers after cessation of antiretroviral therapy. Sci Transl Med *13*. 10.1126/scitranslmed.abg3071.

6. Lim, S.Y., Osuna, C.E., Hraber, P.T., Hesselgesser, J., Gerold, J.M., Barnes, T.L., Sanisetty, S., Seaman, M.S., Lewis, M.G., Geleziunas, R., Miller, M.D., et al. (2018). TLR7 agonists induce transient viremia and reduce the viral reservoir in SIV-infected rhesus macaques on antiretroviral therapy. Sci Transl Med *10*. 10.1126/scitranslmed.aao4521.

7. Borducchi, E.N., Liu, J., Nkolola, J.P., Cadena, A.M., Yu, W.H., Fischinger, S., Broge, T., Abbink, P., Mercado, N.B., Chandrashekar, A., Jetton, D., et al. (2018). Antibody and TLR7 agonist delay viral rebound in SHIV-infected monkeys. Nature *563*, 360–364. 10.1038/s41586-018-0600-6.

8. Korolowizc, K.E., Li, B., Huang, X., Yon, C., Rodrigo, E., Corpuz, M., Plouffe, D.M., Kallakury, B.V., Suresh, M., Wu, T.Y., Miller, A.T., et al. (2019). Liver-Targeted Toll-Like Receptor 7 Agonist Combined With Entecavir Promotes a Functional Cure in the Woodchuck Model of Hepatitis B Virus. Hepatol Commun *3*, 1296–1310. 10.1002/hep4.1397.

9. Lanford, R.E., Guerra, B., Chavez, D., Giavedoni, L., Hodara, V.L., Brasky, K.M., Fosdick, A., Frey, C.R., Zheng, J., Wolfgang, G., Halcomb, R.L., et al. (2013). GS-9620, an oral agonist of Toll-like receptor-7, induces prolonged suppression of

854 hepatitis B virus in chronically infected chimpanzees. Gastroenterology *144*, 1508–
855 1517, 1517 e1501–1510. 10.1053/j.gastro.2013.02.003.
856 10. Menne, S., Tumas, D.B., Liu, K.H., Thampi, L., AlDeghaither, D., Baldwin,
857 B.H., Bellezza, C.A., Cote, P.J., Zheng, J., Halcomb, R., Fosdick, A., et al. (2015).
858 Sustained efficacy and seroconversion with the Toll–like receptor 7 agonist GS–
859 9620 in the Woodchuck model of chronic hepatitis B. J Hepatol *62*, 1237–1245.
860 10.1016/j.jhep.2014.12.026.
861 11. Lopatin, U., Wolfgang, G., Tumas, D., Frey, C.R., Ohmstede, C.,
862 Hesselgesser, J., Kearney, B., Moorehead, L., Subramanian, G.M., and McHutchison,
863 J.G. (2013). Safety, pharmacokinetics and pharmacodynamics of GS–9620, an oral
864 Toll–like receptor 7 agonist. Antivir Ther *18*, 409–418. 10.3851/IMP2548.
865 12. Gane, E.J., Lim, Y.S., Gordon, S.C., Visvanathan, K., Sicard, E., Fedorak,
866 R.N., Roberts, S., Massetto, B., Ye, Z., Pflanz, S., Garrison, K.L., et al. (2015). The
867 oral toll–like receptor–7 agonist GS–9620 in patients with chronic hepatitis B virus
868 infection. J Hepatol *63*, 320–328. 10.1016/j.jhep.2015.02.037.
869 13. Janssen, H.L.A., Brunetto, M.R., Kim, Y.J., Ferrari, C., Massetto, B.,
870 Nguyen, A.H., Joshi, A., Woo, J., Lau, A.H., Gaggar, A., Subramanian, G.M., et al.
871 (2018). Safety, efficacy and pharmacodynamics of vesatolimod (GS–9620) in
872 virally suppressed patients with chronic hepatitis B. J Hepatol *68*, 431–440.
873 10.1016/j.jhep.2017.10.027.
874 14. Messaoudi, I., Estep, R., Robinson, B., and Wong, S.W. (2011).
875 Nonhuman primate models of human immunology. Antioxid Redox Signal *14*, 261–
876 273. 10.1089/ars.2010.3241.
877 15. Takahama, S., Ishige, K., Nogimori, T., Yasutomi, Y., Appay, V., and
878 Yamamoto, T. (2023). Model for predicting age–dependent safety and
879 immunomodulatory effects of STING ligands in non–human primates. Mol Ther
880 Methods Clin Dev *28*, 99–115. 10.1016/j.omtm.2022.12.008.
881 16. Shigeno, S., Kodama, T., Murai, K., Motooka, D., Fukushima, A., Nishio,
882 A., Hikita, H., Tatsumi, T., Okamoto, T., Kanto, T., and Takehara, T. (2025).
883 Intrahepatic Exhausted Antiviral Immunity in an Immunocompetent Mouse Model
884 of Chronic Hepatitis B. Cell Mol Gastroenterol Hepatol *19*, 101412.
885 10.1016/j.jcmgh.2024.101412.
886 17. Ota, Y., Nagai, Y., Hirose, Y., Hori, S., Koga–Yamakawa, E., Eguchi, K.,
887 Sumida, K., Murata, M., Umehara, H., and Yamamoto, S. (2023). DSP–0509, a

systemically available TLR7 agonist, exhibits combination effect with immune checkpoint blockade by activating anti-tumor immune effects. Front Immunol *14*, 1055671. 10.3389/fimmu.2023.1055671.

18. Ota, Y., Inagaki, R., Sumida, K., Nakamura, M., Nagai, Y., and Yamamoto, S. (2024). DSP-0509, a TLR7 agonist, exerted synergistic anti-tumor immunity combined with various immune therapies through modulating diverse immune cells in cancer microenvironment. Front Oncol *14*, 1410373. 10.3389/fonc.2024.1410373.

19. Ota, Y., Inagaki, R., Nagai, Y., Hirose, Y., Murata, M., and Yamamoto, S. (2024). TLR7 agonist, DSP-0509, with radiation combination therapy enhances anti-tumor activity and modulates T cell dependent immune activation. BMC Immunol *25*, 48. 10.1186/s12865-024-00643-x.

20. Du, Y., Wu, J., Liu, J., Zheng, X., Yang, D., and Lu, M. (2022). Toll-like receptor-mediated innate immunity orchestrates adaptive immune responses in HBV infection. Front Immunol *13*, 965018. 10.3389/fimmu.2022.965018.

21. Takahama, S., and Yamamoto, T. (2020). Pattern Recognition Receptor Ligands as an Emerging Therapeutic Agent for Latent HIV-1 Infection. Front Cell Infect Microbiol *10*, 216. 10.3389/fcimb.2020.00216.

22. Li, F., Song, B., Zhou, W.F., and Chu, L.J. (2023). Toll-Like Receptors 7/8: A Paradigm for the Manipulation of Immunologic Reactions for Immunotherapy. Viral Immunol *36*, 564-578. 10.1089/vim.2023.0077.

23. Sun, H., Li, Y., Zhang, P., Xing, H., Zhao, S., Song, Y., Wan, D., and Yu, J. (2022). Targeting toll-like receptor 7/8 for immunotherapy: recent advances and prospectives. Biomark Res *10*, 89. 10.1186/s40364-022-00436-7.

24. Agarwal, K., Ahn, S.H., Elkhashab, M., Lau, A.H., Gaggar, A., Bulusu, A., Tian, X., Cathcart, A.L., Woo, J., Subramanian, G.M., Andreone, P., et al. (2018). Safety and efficacy of vesatolimod (GS-9620) in patients with chronic hepatitis B who are not currently on antiviral treatment. J Viral Hepat *25*, 1331-1340. 10.1111/jvh.12942.

25. Niu, C., Li, L., Daffis, S., Lucifora, J., Bonnin, M., Maadadi, S., Salas, E., Chu, R., Ramos, H., Livingston, C.M., Beran, R.K., et al. (2018). Toll-like receptor 7 agonist GS-9620 induces prolonged inhibition of HBV via a type I interferon-dependent mechanism. J Hepatol *68*, 922-931. 10.1016/j.jhep.2017.12.007.

921 26. Riddler, S.A., Para, M., Benson, C.A., Mills, A., Ramgopal, M., DeJesus, E.,
922 Brinson, C., Cyktor, J., Jacobs, J., Koontz, D., Mellors, J.W., et al. (2021).
923 Vesatolimod, a Toll-like Receptor 7 Agonist, Induces Immune Activation in Virally
924 Suppressed Adults Living With Human Immunodeficiency Virus-1. Clin Infect Dis
925 *72*, e815-e824. 10.1093/cid/ciaa1534.
926 27. Eisenbarth, S.C. (2019). Dendritic cell subsets in T cell programming:
927 location dictates function. Nat Rev Immunol *19*, 89-103. 10.1038/s41577-018-
928 0088-1.
929 28. Gilliet, M., Cao, W., and Liu, Y.J. (2008). Plasmacytoid dendritic cells:
930 sensing nucleic acids in viral infection and autoimmune diseases. Nat Rev Immunol
931 *8*, 594-606. 10.1038/nri2358.
932 29. Yotsuyanagi, H., Kurosaki, M., Yatsuhashi, H., Lee, I.H., Ng, A., Brooks-
933 Rooney, C., and Nguyen, M.H. (2022). Characteristics and Healthcare Costs in the
934 Aging Hepatitis B Population of Japan: A Nationwide Real-World Analysis. Dig Dis
935 *40*, 68-77. 10.1159/000515854.
936 30. Colman, R.J. (2018). Non-human primates as a model for aging.
937 Biochim Biophys Acta Mol Basis Dis *1864*, 2733-2741.
938 10.1016/j.bbadis.2017.07.008.
939 31. Tomiyama, T., Yamamoto, T., Takahama, S., Toshima, T., Itoh, S., Harada,
940 N., Shimokawa, M., Okuzaki, D., Mori, M., and Yoshizumi, T. (2022). Up-regulated
941 LRRN2 expression as a marker for graft quality in living donor liver
942 transplantation. Hepatol Commun *6*, 2836-2849. 10.1002/hep4.2033.
943 32. Panda, A., Qian, F., Mohanty, S., van Duin, D., Newman, F.K., Zhang, L.,
944 Chen, S., Towle, V., Belshe, R.B., Fikrig, E., Allore, H.G., et al. (2010). Age-
945 associated decrease in TLR function in primary human dendritic cells predicts
946 influenza vaccine response. J Immunol *184*, 2518-2527.
947 10.4049/jimmunol.0901022.
948 33. Metcalf, T.U., Cubas, R.A., Ghneim, K., Cartwright, M.J., Grevenynghe,
949 J.V., Richner, J.M., Olagnier, D.P., Wilkinson, P.A., Cameron, M.J., Park, B.S.,
950 Hiscott, J.B., et al. (2015). Global analyses revealed age-related alterations in
951 innate immune responses after stimulation of pathogen recognition receptors.
952 Aging Cell *14*, 421-432. 10.1111/acel.12320.

953

954

955 **Figure legends**

956 **Figure 1. SA-5 safety assessment: Six macaques per dose group were orally**

957 **administered SA-5 at various dose levels to evaluate the effects of multiple**

958 **administrations**

959 (**A**) Structural formula of SA-5, a newly developed orally active TLR7 agonist

960 structurally related to Guretolimod (DSP-0509), a pyrimidine derivative.

961 (**B**) Pie charts indicate the proportion of main subsets in blood. To accommodate space

962 constraints, time points are abbreviated as d0, d1, and d7, corresponding to day 0, day 1,

963 and day 7, respectively. (**C**) Box plots indicate the changes in blood CRP level (day 0,

964 1, 7) after administration measured by biochemical test. (**D**) Box plots indicate the

965 changes in blood AST level (day 0, 1, 7) after administration measured by biochemical

966 test. (**E**) Box plots indicate the changes in the frequency of intermediate monocytes (day

967 0, 1, 7) after administration measured by flow cytometry. (**F**) Box plots indicate the

968 changes in the activation of intermediate monocytes (day 0, 1, 7) after administration

969 measured by flow cytometry. (**C**, **D**, **E**, **F**) Colors indicate doses described in the legend

970 of **B**. Statistical significance relative to day 0 in each administration was determined

971 using paired Wilcoxon tests followed by Benjamini–Hochberg false discovery rate

(FDR) correction across dose groups within each administration and time point; adjusted *q*-values are shown. Unless noted otherwise, adjusted *q*-values are denoted as: *** $q < 0.001$, ** $q < 0.01$, * $q < 0.05$. (**G**) Box plots indicate the changes in the frequency of intermediate monocytes (day 0 at Ad.01 vs day 7 at Ad.12). (**H**) Box plots indicate the changes in the activation of intermediate monocytes (day 0 at Ad.01 vs day 7 at Ad.12). (**G**, **H**) Colors indicate groups as described in the legend of **G**. Statistical significance was determined using the paired Mann-Whitney *U* test comparing Ad.12 day 7 with Ad.01 day 0 (*$p < 0.05$, **$p < 0.01$; ns, not significant).

Abbreviations for Figure 1:

AST, aspartate aminotransferase; IL-6, interleukin-6; ELISA, enzyme-linked immunosorbent assay; iMo, intermediate monocytes; FCM, flow cytometry; dpa, days post-administration; CBC, complete blood count; CRP, C-reactive protein.

Figure 2. Multiparameter safety assessment of multiple SA-5 administration of different doses in cynomolgus macaque

(**A**) Schematic depiction of the analysis pipeline. (**B**) Principal component analysis (PCA) plot generated using values of selected parameters based on the statistically significant data shown in Figure S9. Probability ellipses indicate the area where 90 percent of a distribution lies. The colors indicate the dose. (**C**) Bar plots indicate the relative size of the ellipse area shown in **B**. Colors indicate each dose. (**D**) PCA plot generated using values of selected parameters based on the statistically significant data. Colors indicate each dose as in **B**.

Abbreviations for Figure 2:

PCA, principal component analysis; PC1, principal component 1.

Figure 3. Efficacy assessment of multiple SA-5 administration of different doses in cynomolgus macaque

Six macaques per dose were orally administrated with SA-5 as indicated.

(**A**) Box plots indicate the changes in plasma IFN-α level (day 0, 1, 7) after administration measured by ELISA. (**B**) Box plots indicate the changes in plasma IFN-α level (day 0 at Ad.01 vs. day 7 at Ad.12). (**C**) Box plots indicating representative changes in IFN-induced gene expression (days 0, 1, and 7) after administration as

measured by qRT-PCR. (**D**) Box plots indicating representative changes in IFN-induced gene expression (day 0 at Ad.01 vs. day 7 at Ad.12). (**E**) Box plots indicate changes in DC activation ($CD80^+$ frequency) (days 0, 1, and 7) after administration, as measured by flow cytometry. (**F**) Box plots indicating the changes in DC activation (CD80 MFI in pDC) (days 0, 1, and 7) after administration, measured by flow cytometry. (**G**) Box plots indicate the changes in DC activation ($CD80^+$ frequency) (day 0 at Ad.01 vs. day 7 at Ad.12). (**H**) Box plots indicate the changes in DC activation (CD80 MFI in pDC) (day 0 at Ad.01 vs. day 7 at Ad.12). (**I**) Scatterplot showing the correlation between IFN-α and CD80 MFI in pDC at 1 dpa, including data from all administrations (Ad.01–Ad.12), thereby increasing statistical power. (**A**, **C**, **E**, **F**) Colors indicate each dose. Statistical significance relative to day 0 in each administration was determined using paired Wilcoxon tests followed by Benjamini–Hochberg false discovery rate (FDR) correction across dose groups within each administration and time point; adjusted *q*-values are shown. Unless noted otherwise, adjusted *q*-values are denoted as: *** $q < 0.001$, ** $q < 0.01$, * $q < 0.05$. (**B**, **D**, **G**, **H**) Statistical significance was determined by paired Mann-Whitney *U* test comparing Ad.12 day 7 with Ad.01 day 0

(*$p < 0.05$, **$p < 0.01$; ns, not significant). (**I**) Correlation was evaluated using the Spearman's rank correlation test. Colors indicate each dose as described in **A**.

Abbreviations for Figure 3:

IFN-α, interferon-alpha; qRT-PCR, quantitative reverse transcription PCR; pDC, plasmacytoid dendritic cell; MFI, median fluorescence intensity; ISG, interferon-stimulated gene; IFIT1, interferon-induced protein with tetratricopeptide repeats 1.

Figure 4. Multiparameter efficacy assessment of multiple SA-5 administration of different doses in cynomolgus macaque

(**A**) Schematic depiction of the analysis pipeline. (**B**) Principal component analysis (PCA) plot generated using values of selected parameters based on the statistically significant data shown in **Figure 2C**. Probability ellipses indicate the area where 90 percent of a distribution lies. The colors indicate the dose. (**C**) Bar plots indicate the relative size of the ellipse area shown in **D**. Colors indicate each dose as in **B**. (**D**) PCA plot generated using values of selected parameters based on the statistically significant data shown in **Figure 2C**. The colors indicate the dose.

Abbreviations for Figure 4:

PCA, principal component analysis; ISG, interferon-stimulated gene; IFN-α, interferon-alpha.

Figure 5. Integrated analysis of safety and efficacy

(**A**) Scatter plot indicates PC1 values from two principal component analyses (PCAs) for safety and efficacy. Probability ellipses indicate areas encompassing 90% of the distribution. Dashed lines indicate the boundaries of four regions defined by the ellipse border at 1 mg/kg. Colors indicate each dose. (**B**) PC1-safety values in each dose group. (**C**) PC1-efficacy values in each dose group. (**D**) Scatter indicates PC1 values for safety and efficacy, as in **A**, but not separated by dose. Colors indicate each region. (**E**) Bar plots indicate the frequency of macaques in each region as in **D**. (**F**) CRP scores in each dose group. (**G**) IFN-α scores in each dose group. (**H**) Scatter plot indicates the correlation between CRP values at Ad.01 and Ad.12. (**I**) Scatter plot indicates the correlation between IFN-α values at Ad.01 and Ad.12. **(B, C)** Statistical significance among dose groups was determined using the Wilcoxon rank-sum test stratified by administration (Van Elteren), comparing each dose group with the 1 mg/kg group. **(F, G)** Statistical significance among dose groups based on fold-change values at day 1

(relative to day 0) was determined using the same test. *P* values were adjusted for multiple comparisons among dose groups using the Benjamini–Hochberg false discovery rate (FDR) correction; adjusted *q*-values are shown. Unless noted otherwise, adjusted *q*-values are denoted as: *** $q < 0.001$, ** $q < 0.01$, * $q < 0.05$. (**H, I**) Statistical significance was determined using the Spearman's rank correlation test. (**A**–**C**, **F**, **G**) Colors indicate each dose as in **A**. (**D**, **E**) Colors indicate each region as in **D**.

Abbreviations for Figure 5:

PCA, principal component analysis; PC1, principal component 1; CRP, C-reactive protein; IFN-α, interferon-alpha.

Figure 6. Direct comparison of SA-5 vs. GS-9620

(**A**) Line plots indicate changes in blood CRP levels (day 0, 1, 7) after administration, measured by biochemical testing. (**B**) Line plots indicate changes in plasma IFN-α levels (day 0, 1, 7) after administration, measured by ELISA. (**C**) Scatter plot indicates PC1 values from two principal component analyses (PCAs) for safety and efficacy. Probability ellipses indicate areas encompassing 90% of the distribution. Dashed lines indicate the borders of the four regions defined in **Figure 5**. Colors indicate the

adjuvant. (**D**) PC1-safety values in each adjuvant group. (**E**) PC1-efficacy values in each adjuvant group. (**F**) Bar plots indicate the frequency of macaques in each region as in **Figure 5E**. (**G**) CRP scores in each adjuvant group. (**H**) IFN-α scores in each adjuvant group. (**A**, **B**) Statistical significance was determined using the paired Mann–Whitney *U* test for comparisons with day 0. Blue asterisks indicate comparisons with day 0 of Administration 1 (Ad.01), and red asterisks indicate comparisons with day 0 of each corresponding administration. (*$p < 0.05$). (**D**, **E**, **G**, **H**) Statistical significance was determined using the Mann–Whitney *U* test for comparisons between GS-9620 and SA-5 at each corresponding time point (*$p < 0.05$, **$p < 0.01$, ***$p < 0.001$, ****$p < 0.0001$). (**C**–**E**, **G**, **H**) Colors indicate each adjuvant as in **C**. (**F**) Colors indicate each region as in **Figure 5E**.

Abbreviations for Figure 6:

PCA, principal component analysis; CRP, C-reactive protein; IFN-α, interferon-alpha; PC1, principal component 1.

Figure 7. Direct comparison of young vs. older populations

(**A**) Line plots indicate changes in blood CRP levels (day 0, 1, 7) after administration, measured by biochemical testing. (**B**) Line plots indicate changes in plasma IFN-α levels (day 0, 1, 7) after administration, measured by ELISA. (**C**) Scatter plot indicates PC1 values from two principal component analyses (PCAs) for safety and efficacy. Probability ellipses indicate areas encompassing 90% of the distribution. Dashed lines indicate the borders of the four regions defined in **Figure 5**. (**D**) PC1-safety values in each age group. (**E**) PC1-efficacy values in each age group. (**F**) Bar plots indicate the frequency of macaques in each region as in **Figure 5E**. (**G**) CRP scores in each age group. (**H**) IFN-α scores in each age group. (**A**, **B**) Statistical significance was determined using the paired Mann–Whitney *U* test for comparisons with day 0. Blue asterisks indicate comparisons with day 0 of Administration 1 (Ad.01), and red asterisks indicate comparisons with day 0 of each corresponding administration. (*$p < 0.05$). (**D**, **E**, **G**, **H**) Statistical significance was determined using the Mann–Whitney *U* test for comparisons between Young and Elder at each corresponding time point (*$p < 0.05$, **$p < 0.01$, ***$p < 0.001$, ****$p < 0.0001$). (**A**–**E**, **G**, **H**) Colors indicate each age group (young vs. older) as in **C**. (**F**) Colors indicate each region as in **Figure 5E**.

Abbreviations for Figure 7:

1105 CRP, C-reactive protein; IFN-α, interferon-alpha; PCA, principal component analysis;

1106 PC1, principal component 1.

1107

Figure. 1

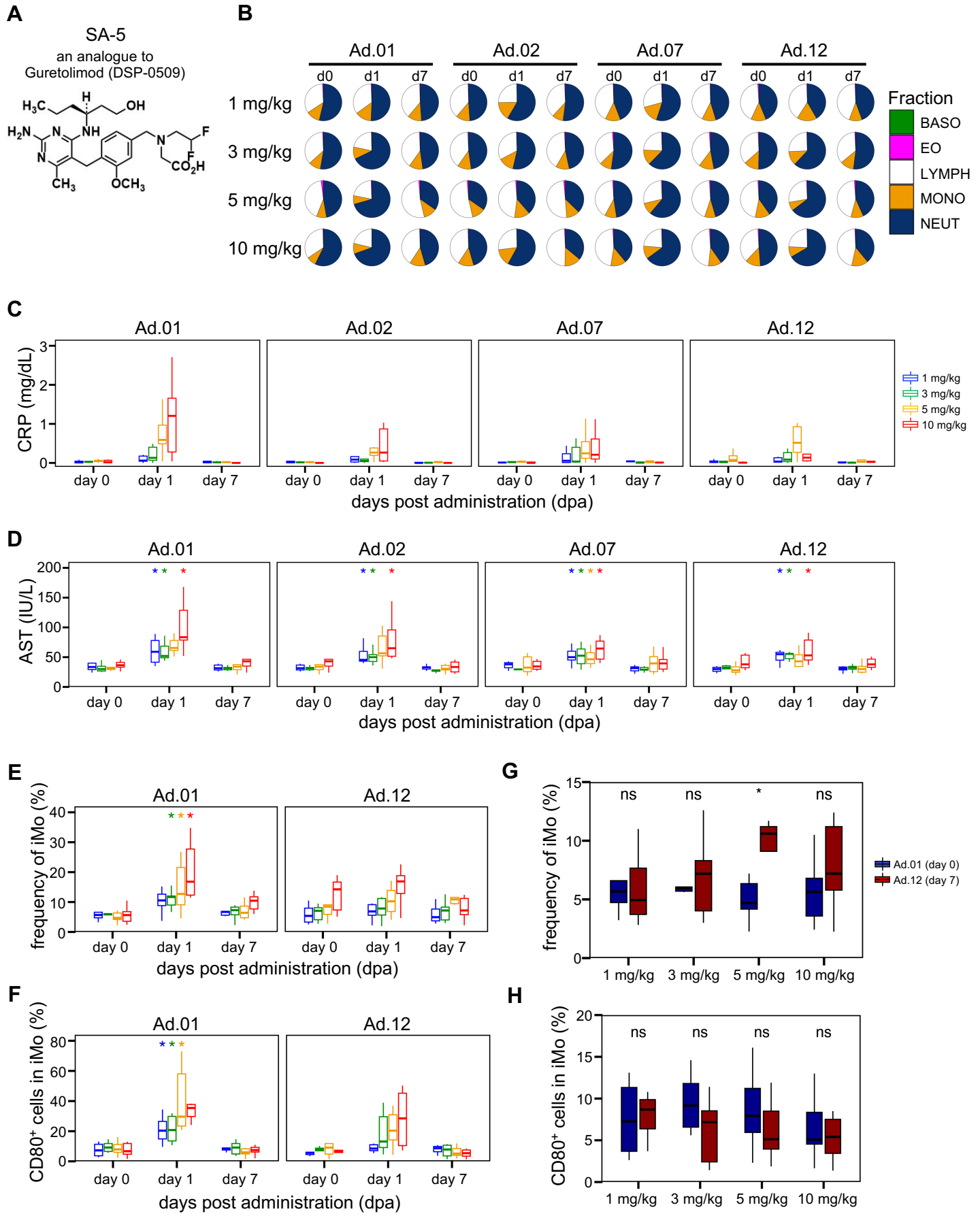
A
SA-5
an analogue to
Guretolimod (DSP-0509)
B
Ad.01
Ad.02
Ad.07
Ad.12
d0
d1
d7
1 mg/kg
3 mg/kg
5 mg/kg
10 mg/kg
Fraction
BASO
EO
LYMPH
MONO
NEUT
C
CRP (mg/dL)
day 0
day 1
day 7
days post administration (dpa)
D
AST (IU/L)
E
frequency of iMo (%)
F
CD80⁺ cells in iMo (%)
G
ns
*
Ad.01 (day 0)
Ad.12 (day 7)
H

Figure. 2

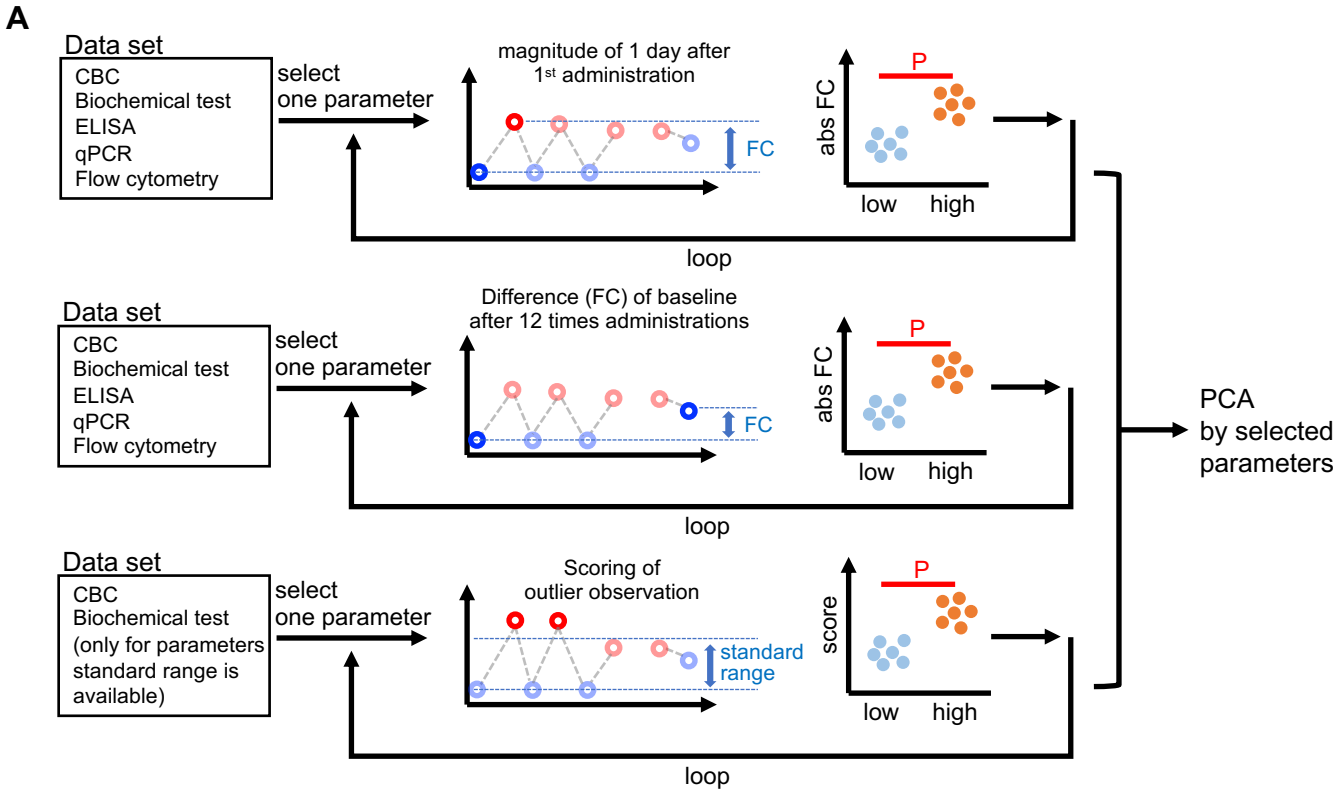
A
Data set
CBC
Biochemical test
ELISA
qPCR
Flow cytometry
select
one parameter
magnitude of 1 day after
1st administration
FC
abs FC
P
low
high
loop
Data set
CBC
Biochemical test
ELISA
qPCR
Flow cytometry
select
one parameter
Difference (FC) of baseline
after 12 times administrations
FC
abs FC
P
low
high
loop
Data set
CBC
Biochemical test
(only for parameters
standard range is
available)
select
one parameter
Scoring of
outlier observation
standard
range
score
P
low
high
loop
PCA
by selected
parameters

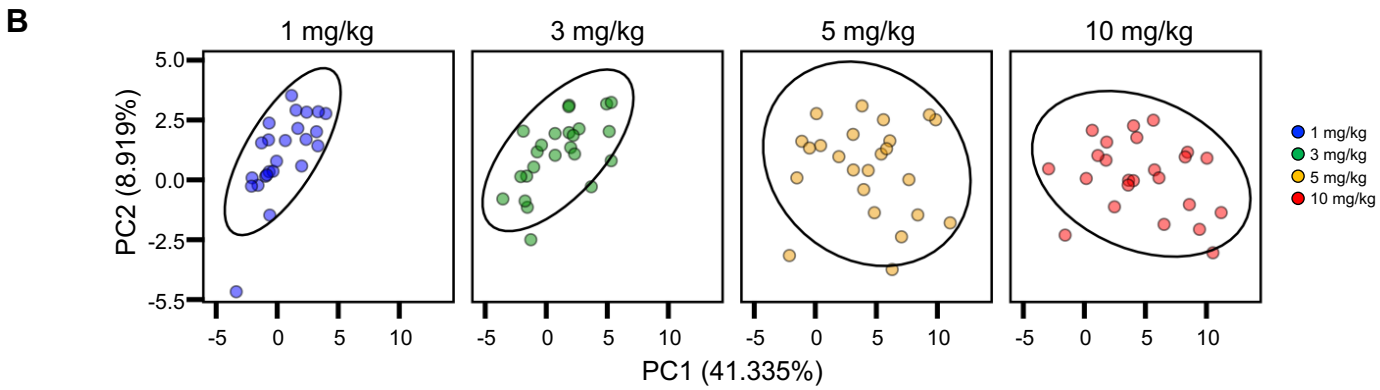
B
1 mg/kg
3 mg/kg
5 mg/kg
10 mg/kg
PC2 (8.919%)
PC1 (41.335%)
1 mg/kg
3 mg/kg
5 mg/kg
10 mg/kg

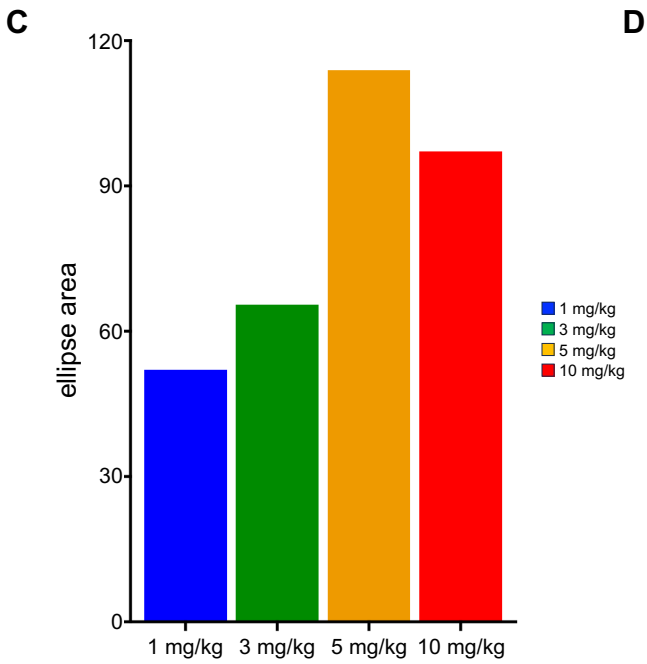
C
ellipse area
1 mg/kg
3 mg/kg
5 mg/kg
10 mg/kg

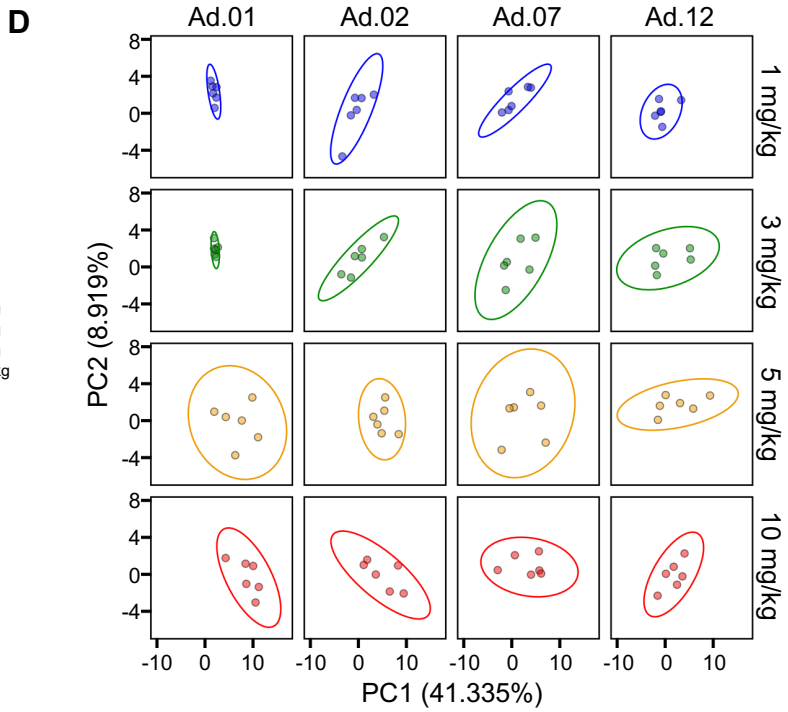
D
Ad.01
Ad.02
Ad.07
Ad.12
1 mg/kg
3 mg/kg
5 mg/kg
10 mg/kg
PC2 (8.919%)
PC1 (41.335%)

Figure. 3

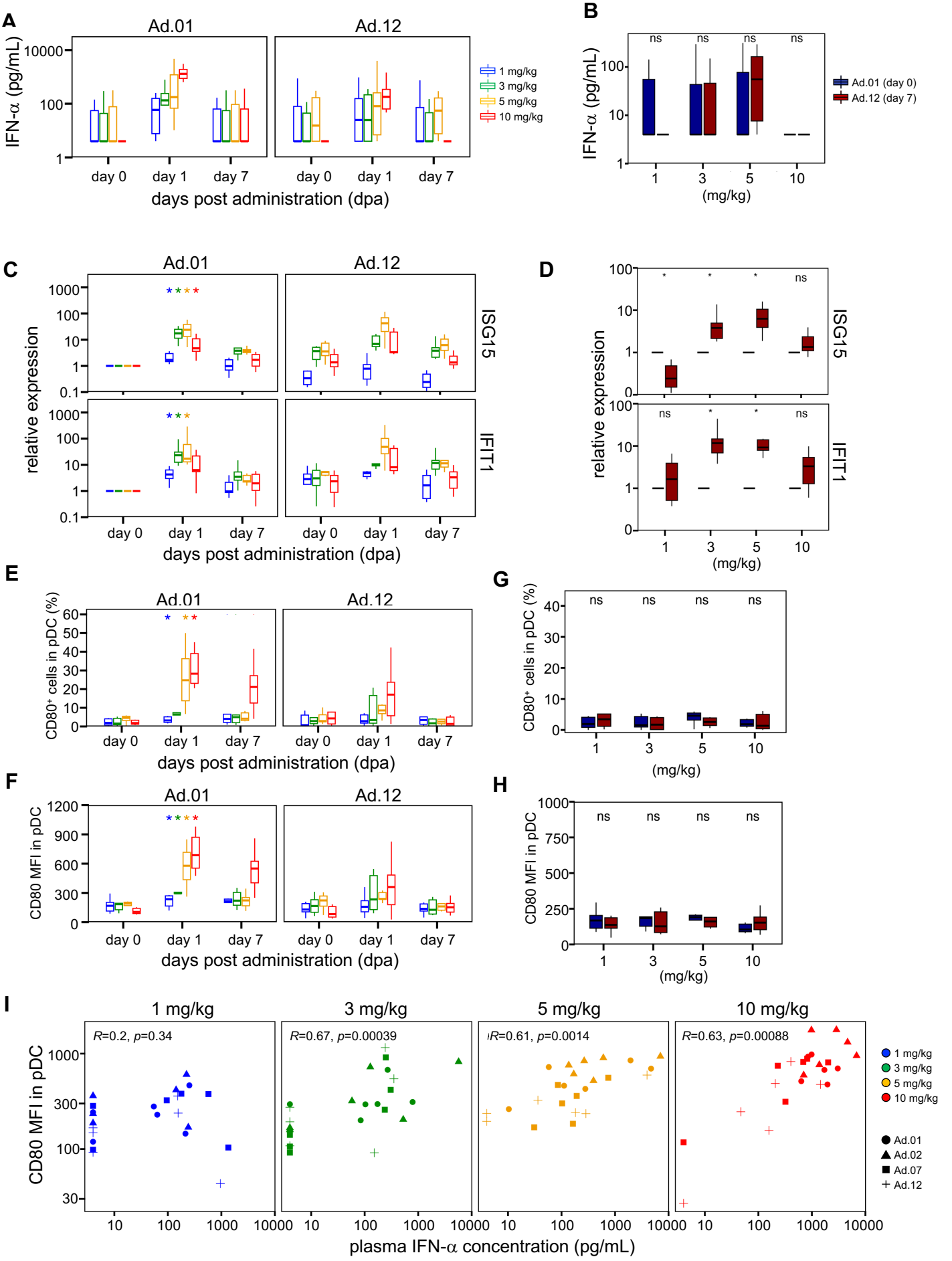
A
Ad.01
Ad.12
IFN-α (pg/mL)
10000
100
1
day 0
day 1
day 7
days post administration (dpa)
1 mg/kg
3 mg/kg
5 mg/kg
10 mg/kg
B
ns
IFN-α (pg/mL)
100
10
1
1
3
5
10
(mg/kg)
Ad.01 (day 0)
Ad.12 (day 7)
C
Ad.01
Ad.12
relative expression
1000
100
10
1
0.1
ISG15
IFIT1
day 0
day 1
day 7
days post administration (dpa)
D
relative expression
100
10
1
0
ns
ISG15
IFIT1
1
3
5
10
(mg/kg)
E
Ad.01
Ad.12
CD80⁺ cells in pDC (%)
60
50
40
30
20
10
0
day 0
day 1
day 7
days post administration (dpa)
G
CD80⁺ cells in pDC (%)
40
30
20
10
0
ns
1
3
5
10
(mg/kg)
F
Ad.01
Ad.12
CD80 MFI in pDC
1200
900
600
300
0
day 0
day 1
day 7
days post administration (dpa)
H
CD80 MFI in pDC
1000
750
500
250
0
ns
1
3
5
10
(mg/kg)
I
1 mg/kg
3 mg/kg
5 mg/kg
10 mg/kg
R=0.2, p=0.34
R=0.67, p=0.00039
R=0.61, p=0.0014
R=0.63, p=0.00088
CD80 MFI in pDC
1000
300
100
30
10
100
1000
10000
plasma IFN-α concentration (pg/mL)
1 mg/kg
3 mg/kg
5 mg/kg
10 mg/kg
Ad.01
Ad.02
Ad.07
Ad.12

Figure. 4

A

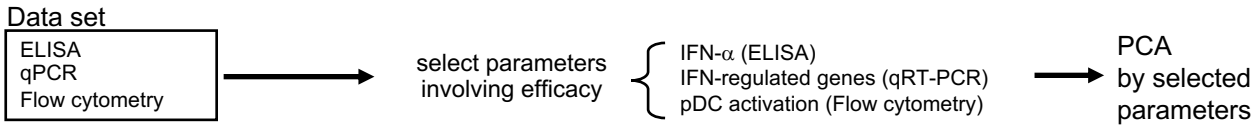

B

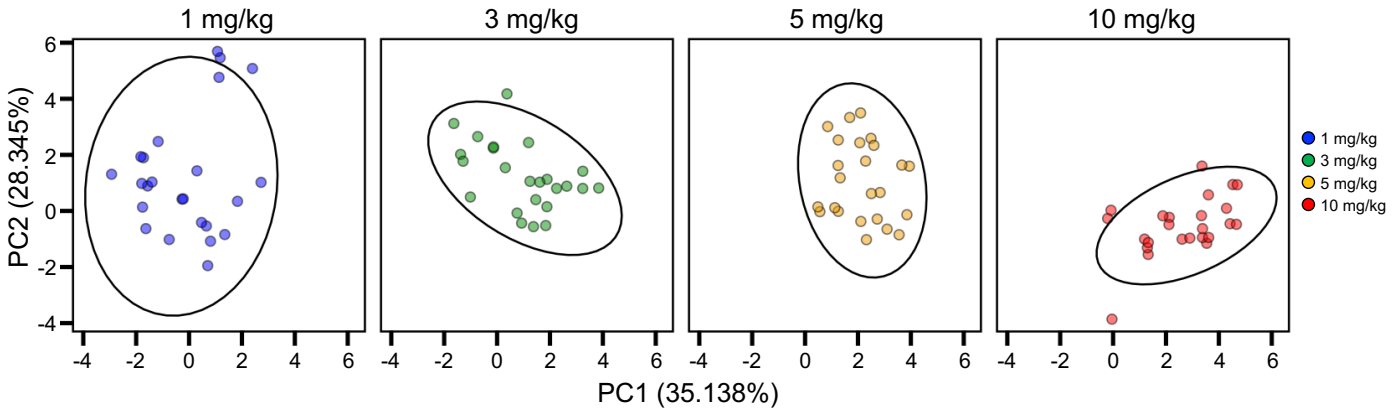

C

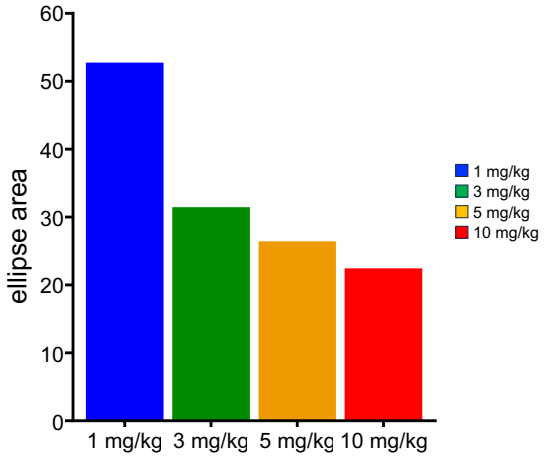

D

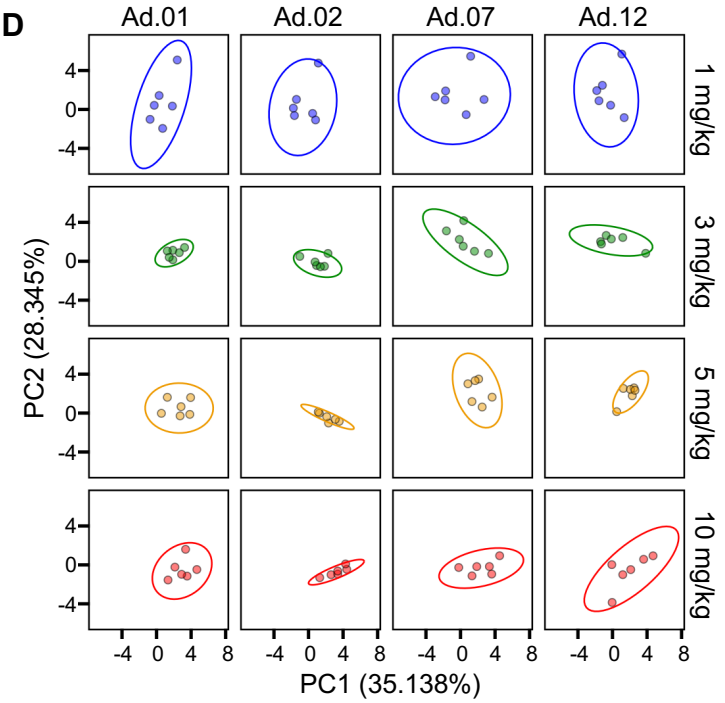

Figure. 5

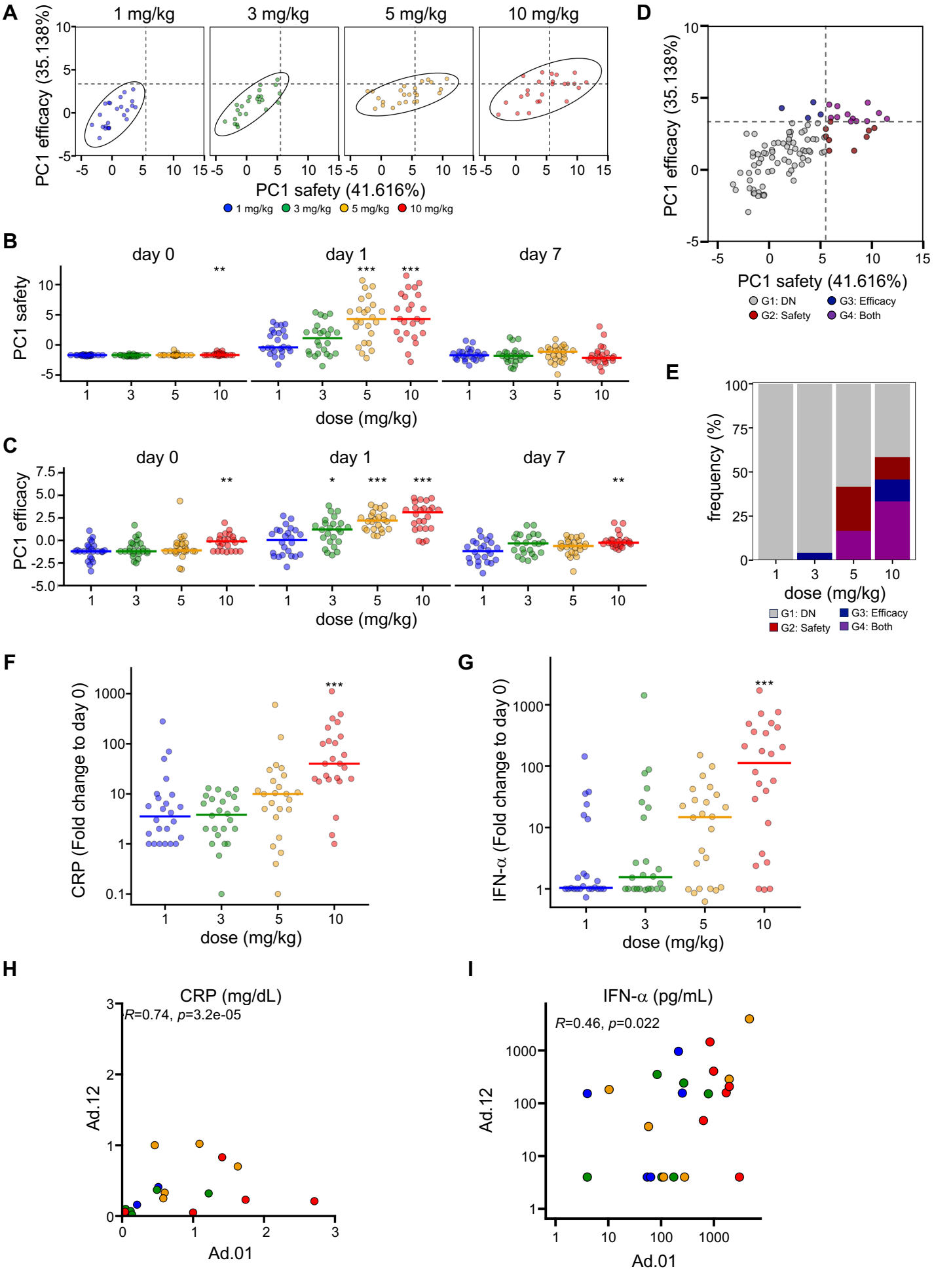
A
1 mg/kg
3 mg/kg
5 mg/kg
10 mg/kg
PC1 efficacy (35.138%)
PC1 safety (41.616%)
1 mg/kg 3 mg/kg 5 mg/kg 10 mg/kg
B
day 0
day 1
day 7
PC1 safety
dose (mg/kg)
C
day 0
day 1
day 7
PC1 efficacy
dose (mg/kg)
D
PC1 efficacy (35.138%)
PC1 safety (41.616%)
G1: DN
G2: Safety
G3: Efficacy
G4: Both
E
frequency (%)
dose (mg/kg)
G1: DN
G2: Safety
G3: Efficacy
G4: Both
F
CRP (Fold change to day 0)
dose (mg/kg)
G
IFN-α (Fold change to day 0)
dose (mg/kg)
H
CRP (mg/dL)
R=0.74, p=3.2e-05
Ad.12
Ad.01
I
IFN-α (pg/mL)
R=0.46, p=0.022
Ad.12
Ad.01

Figure. 6

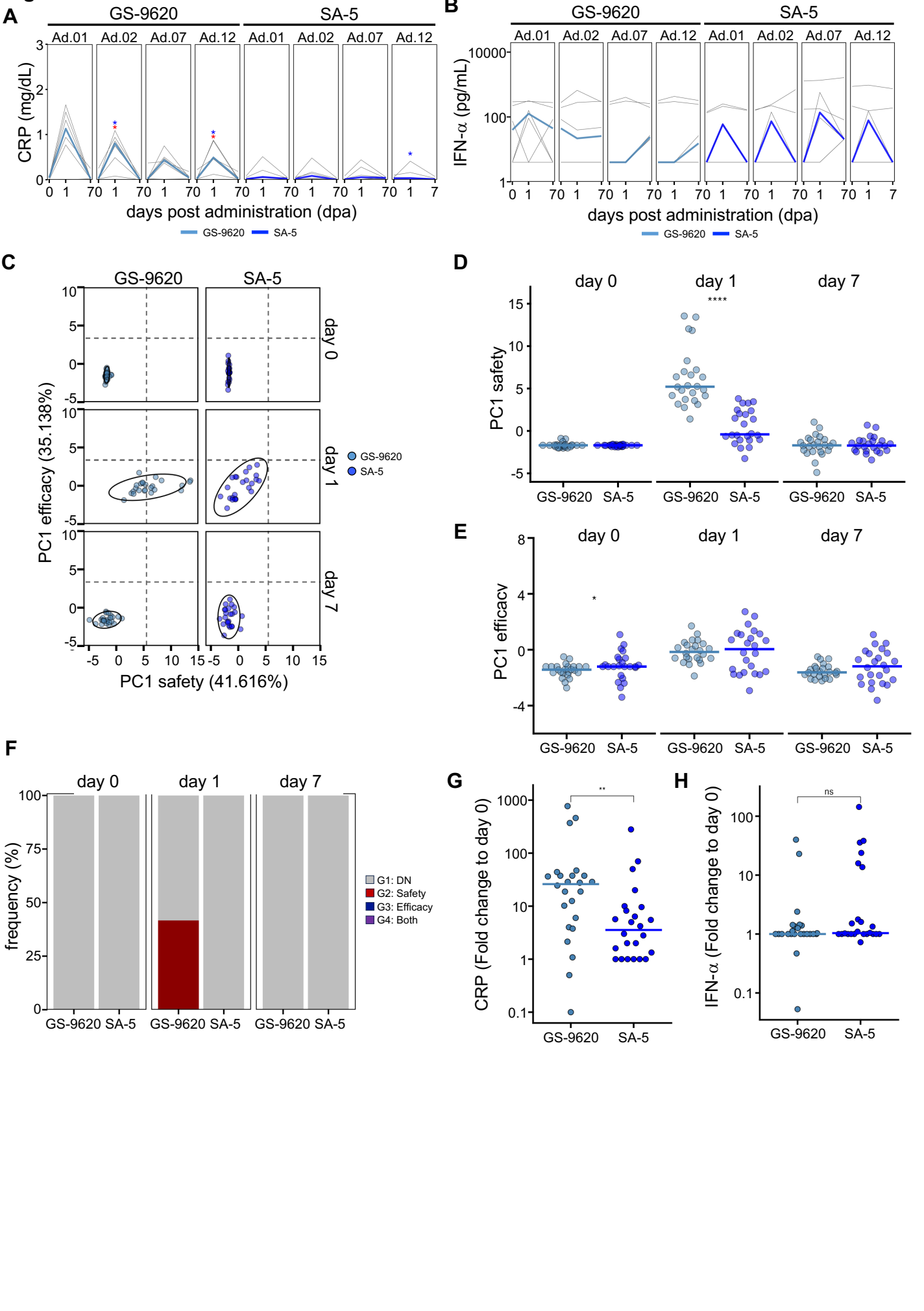
A
GS-9620
SA-5
Ad.01
Ad.02
Ad.07
Ad.12
CRP (mg/dL)
days post administration (dpa)
GS-9620
SA-5
B
IFN-α (pg/mL)
C
PC1 efficacy (35.138%)
PC1 safety (41.616%)
day 0
day 1
day 7
D
PC1 safety
E
PC1 efficacy
F
frequency (%)
G1: DN
G2: Safety
G3: Efficacy
G4: Both
G
CRP (Fold change to day 0)
H
IFN-α (Fold change to day 0)
ns

Figure. 7

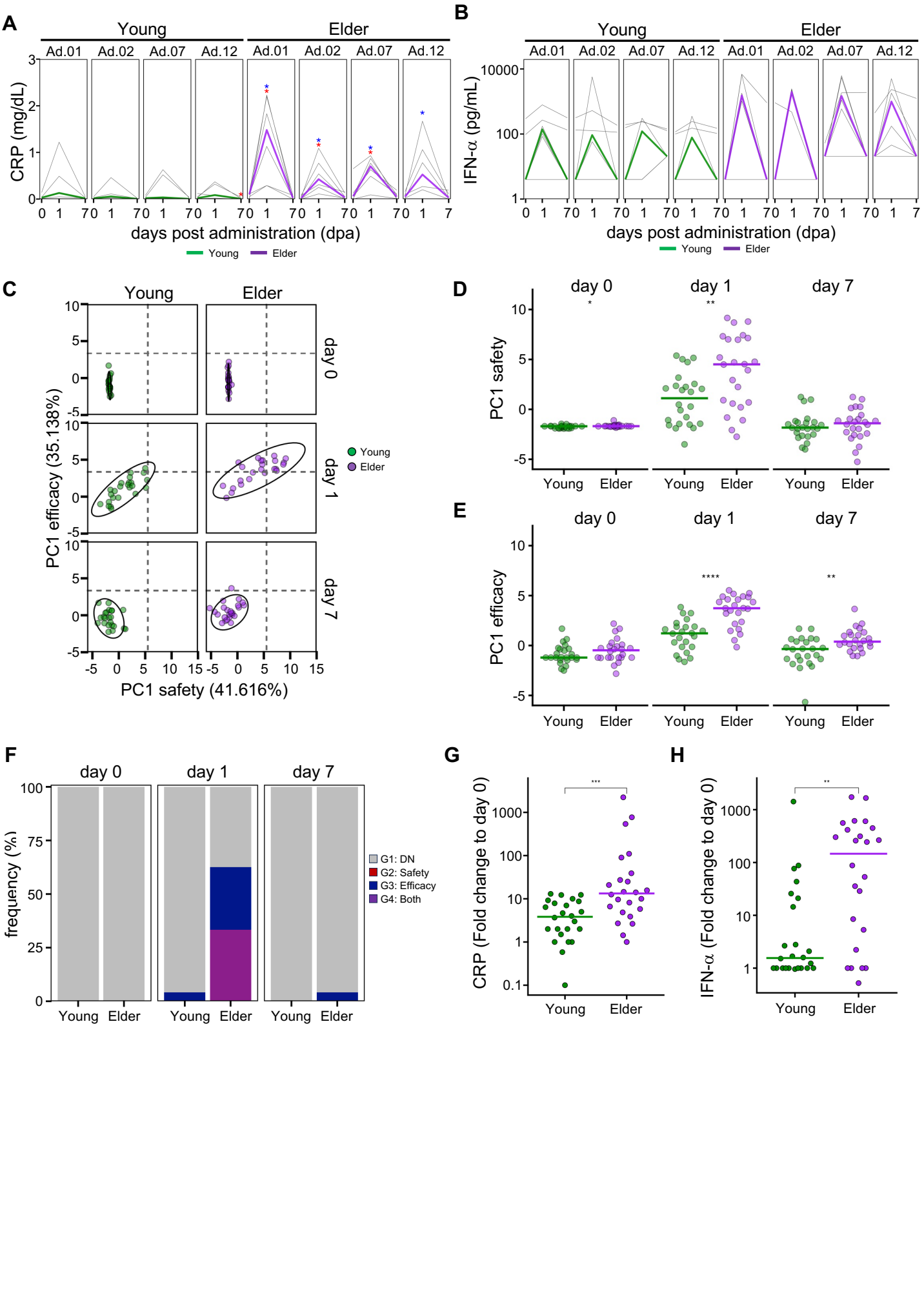
A
Young
Elder
Ad.01
Ad.02
Ad.07
Ad.12
CRP (mg/dL)
days post administration (dpa)
Young
Elder
B
IFN-α (pg/mL)
C
PC1 efficacy (35.138%)
PC1 safety (41.616%)
day 0
day 1
day 7
D
PC1 safety
E
PC1 efficacy
F
frequency (%)
G1: DN
G2: Safety
G3: Efficacy
G4: Both
G
CRP (Fold change to day 0)
H
IFN-α (Fold change to day 0)